REPORT DOCUMENTATION PAGE

Form Approved
OMB No. 0704-0188

1. AGENCY USE ONLY (Leave blank)	2. REPORT DATE	3. REPORT TYPE AND DATES COVERED
	Mar96	Final - 01Jan87-31Dec88

4. TITLE AND SUBTITLE
Ice Vibrations on the Arctic Channel

5. FUNDING NUMBERS
N00014-87-K-0274

6. AUTHOR(S)
H. Kutschale

7. PERFORMING ORGANIZATION NAME(S) AND ADDRESS(ES)
The Trustees of Columbia University in the City of N Y
Box 20 - Low Memorial Library
New York, N Y 10027

8. PERFORMING ORGANIZATION REPORT NUMBER
5-21644

9. SPONSORING / MONITORING AGENCY NAME(S) AND ADDRESS(ES)
Office of Naval Research
Ballston Tower One
800 North Quincy St.
Arlington, VA 22217-5660

10. SPONSORING / MONITORING AGENCY REPORT NUMBER

11. SUPPLEMENTARY NOTES
The view, opinions and/or findings contained in this report are those of the author(s) and should not be construed as an official Department of the Army position, policy, or decision, unless so designated by other documentation.

12a. DISTRIBUTION / AVAILABILITY STATEMENT
Approved for public release; distribution unlimited.

12b. DISTRIBUTION CODE

13. ABSTRACT (Maximum 200 words)

Differences in signal-to-noise ratios between hydrophones and geophones were measured as a function of signal grazing angle with level ice and signal frequency. The frequency distributions in the differences clearly show two groupings. One group represents waves traveling in the Arctic sound channel with grazing angles less than 20 degrees and the other group represents waves with large grazing angles beyond 70 degrees such as long-range mantle P and S waves created by earthquakes and explosions. In the band 8 Hz to 20 Hz in SOFAR signals, T-phases, and topographic echoes the hydrophones at depths near 40 m in the water of the channel record waves about 7 dB stronger in average signal-to-noise ratio compared to vertical geophones on the ice. At large grazing angles near 75 degrees the relative performance between the two sensors reverses, with the average signal-to-noise ratio recorded by the vertical geophones about 3 dB better compared to that recorded by the hydrophones.

14. SUBJECT TERMS	15. NUMBER OF PAGES
Arctic SOFAR signals, geophones, hydrophones, Arctic channel	16. PRICE CODE

17. SECURITY CLASSIFICATION OF REPORT	18. SECURITY CLASSIFICATION	19. SECURITY CLASSIFICATION OF ABSTRACT	20. LIMITATION OF ABSTRACT
UNCLASSIFIED	UNCLASSIFIED	UNCLASSIFIED	UL

DISCLAIMER NOTICE

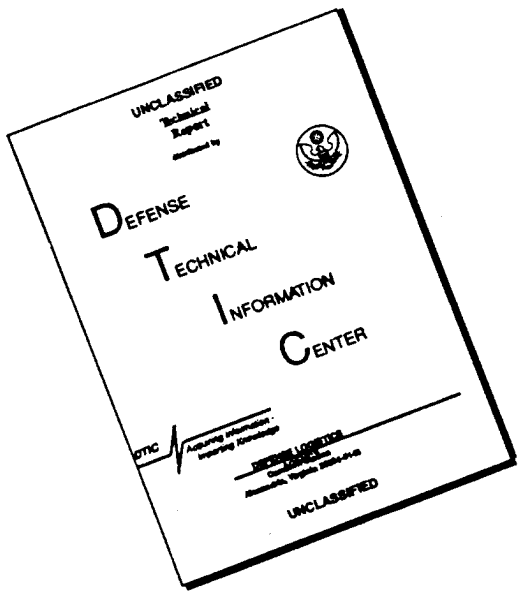

THIS DOCUMENT IS BEST QUALITY AVAILABLE. THE COPY FURNISHED TO DTIC CONTAINED A SIGNIFICANT NUMBER OF PAGES WHICH DO NOT REPRODUCE LEGIBLY.

Ice Vibrations on the Arctic Channel

by

Henry W. Kutschale

Lamont-Doherty Earth Observatory
of Columbia University

Palisades, New York 10964

Work Supported By

Office of Naval Research
Arlington, Virginia 22217

Under Contract N00014-87-K-0274

January 1, 1987 - December 31, 1988

Final Report N00014-87-K-0274
Henry W. Kutschale

Abstract

Differences in signal-to-noise ratios recorded concurrently by hydrophones and by geophones show a wide range of variation between -10 dB to +20 dB. Thus in some waves traveling through the Arctic channel the vertical geophones on the ice are better listening devices compared to hydrophones at depths of about 40 m to 50 m in the water of the channel.

Differences in signal-to-noise ratios between hydrophones and geophones were measured as a function of signal grazing angle with level ice and signal frequency. The frequency distributions in the differences clearly show two groupings. One group represents waves traveling in the Arctic sound channel with grazing angles less than 20 degrees and the other group represents waves with large grazing angles beyond 70 degrees such as long-range mantle P and S waves created by earthquakes and explosions. At 20 Hz in SOFAR signals, T-phases, and topographic echoes the hydrophones at depths near 40 m in the water of the channel record waves about 7 dB stronger in average signal-to-noise ratio compared to vertical geophones on the ice. At large grazing angles near 75 degrees the relative performance between the two sensors reverses, with the average signal-to-noise ratio recorded by the vertical geophones about 3 dB better compared to that recorded by the hydrophones. The average differences in signal-to-noise ratios between the hydrophones and geophones are nearly independent of frequency in the band from 8 Hz to 20 Hz in both groups of waves. At lower frequencies in both groups of waves the performance of the hydrophones improves relative to the geophones, approaching an average difference of 10 dB at 4 Hz.

Introduction

Our research in Arctic Marine Acoustics has been a strong interplay between field observations and computer modeling of underwater propagation (Ref. 1). During the past 30 years we have completed numerous field experiments of acoustic propagation in the central Arctic Ocean. The resurgence of interest by the Navy in seismic methods of detection of underwater sources in the Arctic channel was spawned by our research in long-range propagation of ice vibrations (Ref. 2). The experiments of the FRAM-TRISTEN series were highly successful, and they provided us with the first opportunity to obtain systematic data of differences of signal-to-noise ratios between hydrophones and geophones as a function of grazing angle with level areas of ice and wave frequency. We also had, for the first time, the opportunity to investigate long-range propagation of ice vibrations created by earthquakes at the Nansen Ridge. The waves created by earthquakes provided important data for the measurements of differences of signal-to-noise ratios concurrently recorded by hydrophones and by geophones. The experiments of the FRAM series complemented earlier experiments of wave propagation recorded by horizontal seismic arrays and a 3-component seismograph with the purpose to measure wave particle motions as a function of horizontal phase velocity (grazing angle), wave frequency and ice thickness.

We believe that seismic methods of detection of sources in the Arctic channel have important applications for Navy operations in the central Arctic Ocean because in some cases the signal-to-noise ratios recorded by geophones are better than those recorded concurrently by hydrophones. Also our data indicate that in general below 75 Hz the spatical coherence is comparable in waves recorded by vertical geophones and by hydrophones. A puzzling feature of the measurements is that the horizontal vibration levels are comparable to the vertical levels, in marked contradiction of present theory, but recent theoretical work conducted at NUSC (Ref. 3) may assist in unscrambling this aspect of the propagation. However, we believe that because of the variability of the ratio of horizontal-to-vertical particle velocity measured from one experiment to the next, a far more complete set of experiments of the type that will be described later must be done.

Simultaneously with the field measurements and the data analysis, we were improving and standardizing our full-wave computer models for transmission loss and pulse propagation to make them as automatic and fool-proof as possible so that we could conveniently analyze the wave propagation. We completed this task with the interim standard codes, and we distributed the combined FFP and normal-mode program (and the corresponding pulse code) to the Navy user groups. These codes, with extended capabilities for the present effort, are used for modeling. A User's Manual of two computer codes is contained in two volumes. These volumes are available as a supplement to this report.

The Arctic SOFAR signals commonly differ markedly in character from those observed in the deep channel, largely because of the predominance of very low frequency waves in the Arctic channel. Waves above 100 Hz are strongly scattered by the rough ice boundaries, and thus they are not propagated within the waveguide to great ranges. Because the wavelengths of the observed waves are commonly comparable with the dimensions of the portion of the duct controlling the propagation, full wave theory must be used to explain the propagation, particularly for propagation of ice vibrations and in general for waves traveling in the upper thousand meters of the water column and for those waves with turning points in the upper 400 m of bottom sediment. The observations of marked frequency dispersion of explosion sounds recorded by hydrophones and by geophones motivated the development of the present computer codes.

Objectives

The objectives of this research are to (1) describe quantitatively by computer modeling the vertical and horizontal ice vibrations observed in experiments on wave propagation in the Arctic channel, (2) analyze measurements of signals and noise recorded concurrently by ice-imbedded geophones and by hydrophones, (3) statistically compare the differences in signal-to-noise ratio between the two sensors, (4) characterize the average signal-to-noise ratio as a function of signal frequency and signal grazing angle, (5) characterize the nature of ice trapped noise, a phenomenon peculiar to ice-embedded geophones, and (6) devise strategies to maximize signal-to-noise ratios recorded by geophones.

Technical Approach

1. Compare measurements of signals and noise recorded concurrently by geophones on the ice and by hydrophones at depth in the water of the channel.

2. Explain the observations by computer modeling of wave propagation.

Geophones Compared to Hydrophones: Signal-To-Noise of Arctic SOFAR Signals

Initial measurements made 30 years ago concurrently with geophones and hydrophones revealed that hydrophones at depths between 38 m and 61 m in the water of the channel displayed a superior signal-to-noise ratio (about 9 DB at 20 Hz) compared to the signal-to-noise ratio of the vertical-component geophones (Ref. 4). The relatively poor performance of the geophones compared to the hydrophones at depth in the channel seems to have discouraged the widespread use of these listening devices for underwater sound in the Arctic channel. However, it was subsequently observed during one series of experiments that the horizontal-radial geophone on the ice surface, with a ratio of signal-to-noise ratios of the geophone to the hydrophone of about 4 DB at 20 Hz, was, in fact, a better listening device for SOFAR signals than a hydrophone at a depth of 30 m in the channel. Because of our previous experience with these listening devices, this result was amazing to us. However, we will demonstrate from a large sample of SOFAR signals (about 500) that occasionally (about two percent of the sample) hydrophones near a depth of 38 m in the channel and geophones on the ice can perform about equally well as listening devices; the seeming contradiction in results between our early measurements and our later ones can be explained by the variation from one experiment to the next in the signal-to-noise ratios measured simultaneously with hydrophones and geophones.

Despite the inferior signal-to-noise ratios of the vertical-component geophones, as compared to the hydrophones, that were observed in the early experiments, the geophones offer two major advantages over the hydrophones.

First, access to the water is not required to deploy the geophones. They can be placed on the ice surface. Thus large numbers of geophones in a seismic array can be deployed rapidly as listening devices on the ice surface. The relative ease of deployment of geophones compared to hydrophones can compensate for the inferior signal-to-noise ratio recorded by a single geophone compared to that recorded by a single hydrophone; this compensation is made by the use of a few more (less than 10) sensors in a seismic array compared to a single underwater hydrophone.

Second, the geophones are not susceptible to cable strum. Cable strum can sometimes be a severe problem in measurements made with hydrophones in the infrasonic frequency band from 1 to 10 Hz.

We will now describe the character of the shot signals recorded by geophones and by hydrophones. Shot signals in the Arctic channel clearly show low-order normal modes. The Arctic SOFAR signals are commonly nearly sinusoidal. This effect is caused by the constructive interference of RSR rays, (Fig. 1), that have traveled in the upper few hundred meters of water, where the sound velocity increases rapidly with depth. Usually, at long-ranges, it is the first two normal modes that are observed in the frequency band below 40 Hz. However, Fig.2 shows that if the channel is deep enough along the entire propagation path, such as over an abyssal plain, the early part of the arriving SOFAR wave train displays a discrete and impulsive character corresponding to the arrivals of deep-penetrating RSR rays, while the latter part of the wave train maintains its nearly sinusoidal character.

The character of the signals is the same regardless of whether they are recorded by a hydrophone or by a geophone. This is shown in Fig. 3 by some typical SOFAR signals created by explosions of five pounds of TNT at various depths in the water of the channel. This is even the case for bottom-interacting signals at phase velocities substantially higher (1.6 to 2.0 km/sec) than those corresponding to the SOFAR signal (Figs. 4a and 4b). An analysis of the wave propagation showed that the velocities of the waves and the frequency dispersion occurring within the wave train were identical in signals detected by both types of sensors. This is as expected, since the frequency equation for phase velocity dispersion is independent of the source and detector. The normal-mode computations showed that the pack ice had a negligible effect on the velocities of the waves and the frequency dispersion of the observed normal-modes.

The dispersive character of the Arctic SOFAR signal is shown in Fig. 5, which is sound spectrogram of a SOFAR signal. The dispersion of waves corresponding to the first and second normal modes is clearly visible in the frequency band below 40 Hz. The impulsive character of the deep-penetrating RSR waves is displayed by horizontal bands across the spectrogram, corresponding to a superposition of many high-order modes with group velocities equal to the mean horizontal velocities of each of the RSR pulses. Agreement between observation and theory is excellent. The group-velocity dispersion of low-order modes in the Arctic channel is very uniform over a long propagation path, but the arrivals of the deep-penetrating RSR waves vary with range in both amplitude and mean horizontal velocity according to their cycle ranges. Because of scattering at the rough boundaries of the ice, only low frequencies can propagate to long distances in the Arctic channel.

In deploying our geophones in the field we have attempted to obtain the best possible recordings at each listening site. Three factors are important in this connection.

First, the geophones are far more sensitive to noise created by local ice deformation than the hydrophones at depth in the channel. In order to minimize the effect of these strong ice vibrations on the detection capabilities of the geophones, we have located them as far as possible from the lateral boundaries of the floe. In other words, we minimized this noise problem by a "sensible siting" of the geophones as far as possible from the noise sources.

Second, the geophones can be more difficult to couple to the medium than the hydrophones. We have been extremely careful in coupling the geophones to the ice to get an undistorted recording of the waves. The summer melt conditions at Station Charlie sometimes proved troublesome to our efforts to keep all elements of the seismic array functioning properly without periodic leveling of the geophones.

Finally, third, the geophones are very sensitive to the man-made ice vibrations created during normal camp operations. (This is the man-made equivalent of noise created by local ice deformation.) Generators, winches, and vehicles all generate strong vibrations which travel efficiently in the ice waveguide. We have mitigated this problem by placing the geophones at least several thousand feet from the main camp or by placing them on a neighboring floe. Pressure ridges and leads strongly attenuate the waves guided by the plate. The measurements discussed in this work were made from recordings in which we are virtually certain that man-made noise was negligible compared to the natural ambient noise.

The relatively poor signal-to-noise ratio of the signals recorded on Station Charlie during the initial experiments by the vertical-component geophones compared to those recorded by the hydrophones seemed reasonable, since the ice can support noise vibrations such as flexural waves and plate compressional waves which are nonexistent or weak in the water in the channel at 38 m (Fig. 6).

On Station Charlie during the initial experiments on SOFAR propagation with geophones as listening devices (Ref. 2), we deployed a two-dimensional horizontal seismic array on the ice in the shape of an "L" with six vertical-component geophones spaced 61 m apart on each leg of the array. The signals were also recorded by a short vertical array of three hydrophones at depths of 15 m, 38 m, and 61 m in the water of the channel. The SOFAR signals created by explosions of 3 to 10 pounds of TNT at depths between 30 and 300 m in the water of the channel traveled about 1100 km across the Canada Basin of the western Arctic Ocean.

With these data recorded in the frequency band from 8 to 25 Hz on photographic paper with an oscillograph, we were able to compare the signal-to-noise ratios measured by geophones to those measured concurrently by hydrophones at depths of 15 m, 38 m and 61 m in the water of the channel. These experiments were conducted over a six-week interval on summer sea ice 3 m thick. For this analysis, we used data recorded by geophones of the seismic array which were the most distant ones form the main camp. At these locations we are virtually certain that man-made noise was negligible compared to the ambient vibrations. The vertical hydrophone array was located far enough from the main camp so that man-made noise was negligible in the water in the band form 8 to 25 Hz. We disregarded any signals when hydrophone cable strum could have contaminated the noise measurements. The signal-to-noise ratio was derived from a noise sample in the band from 8 to 25 Hz immediately preceding the SOFAR signal and from the peak-to-peak amplitude of the waves corresponding to the first normal mode at 20 Hz. From a noise sample at

least 10 to 15 sec in duration, a measurement was made of the average of the envelope of the peak-to-peak amplitudes present for 95 percent of the time in the sample analyzed. The signals were recorded during quiescent intervals between periods of ice deformation that produced ice tremors of the type displayed in Fig. 6.

These experiments showed that the hydrophones are markedly better listening devices compared to the geophone, although there was a significant variability of the differences in ratios for each hydrophone depth.

Since the initial experiments conducted nearly three decades ago, we have recorded over 1500 SOFAR signals. Thus our recordings of SOFAR signals (detected by both geophones and hydrophones) is very extensive. We have virtually basin-wide coverage of the propagation. The experiments include the four seasons of the year. In order to obtain a better estimate of the variability in the differences of signal-to-noise ratios measured from one experiment to the next, we analyzed about 500 pairs of SOFAR signals recorded concurrently by hydrophones and by vertical-component geophones. The signals traveled to ranges of up to about 1300 km. In addition, we listened by ear to about 1000 signals played back from the data tapes at high speed.

The majority of the signals were recorded using nearly identical acquisition systems. The hydrophones of type XU-1333 were designed and made at the Naval Underwater Systems Center. We generally deployed at least two hydrophones, a shallow one near 38 m and a deeper one between 50 and 61 m. These hydrophones are designed to have a flat frequency response in the range from below 1 Hz to 2 kHz. Hydrophone cable fairing was used to reduce cable strum. Geospace HS-10-2 geophones, both vertical and horizontal, were deployed on the ice surface. These geophones have a natural frequency of 2 Hz and were deployed with between 50 to 70 percent critical damping.

The signals were pre-amplified at the ice surface using Ithaco 143 m and 144 m DC powered pre-amplifiers. The signals then passed through some 1-3 km of cable on the ice surface and into a warm lab. Here the signals were again amplified through banks of cascaded Ithaco 451 and 451M amplifiers. Several different gains were recorded, typically 20, 40, 60 and 80 DB, onto magnetic tapes thereby clearly collecting any signal over a wide dynamic range

The signals were recorded onto magnetic tapes in analog format using Hewlett Packard 3964A 4-channel FM instrumentation tape recorders. The signals were recorded in the range of 1 to 156 or 312 Hz, depending on the tape speed used. During the FRAM III and FRAM IV experiments in the eastern Arctic, the ambient noise was also continuously recorded with Sprengnether MEQ 800 seismic drum recorders. Arrival times for the signals, accurate to + 0.25 seconds, were deduced

from the paper records produced. This facilitated the quick location of many signals on the magnetic tapes for eventual data analysis. In the field we also recorded many of the signals on paper with an oscillograph from which we obtained immediately an estimate of the differences of the signal-to-noise ratios recorded by the two types of sensors. These observations agree quite well with the analysis of the signals which we will describe below.

The initial data analysis involved simple amplitude versus time and frequency versus time representations of the signals. Oscillograms of the shot signals were produced by playing the tapes onto a Hewlett-Packard paper recorder. Spectrum analysis was done in real time using a Saicor SA-51 analog spectrum analyzer and displayed onto paper with a Raytheon LSR-910 line scan recorder to identify man-made noise such as that created by a generator, an oceanographic winch, or a vehicle.

In some of the early experiments conducted near ARLIS II and T-3, the entire seismic recording system was initially calibrated using the Wilmer Impedance Bridge technique from which we derived the displacement amplitudes in millimicrons of the signals and the ambient noise field.

The differences of signal-to-noise ratios recorded by the hydrophones and by the geophones were derived from the data recorded on the magnetic tapes in a standard manner similar to that employed in the data recorded with an oscillograph at Stations Charlie and ARLIS II. We chose a hydrophone depth of 125 ft (38 m). The signals were passed through a Khron-Hite band-pass filter (8 to 23 Hz). From samples of tape 3 to 5 minutes in duration immediately preceding the signal, a measurement was made of the average of the envelope of the peak-to-peak amplitudes present for 95 percent of the time in the sample analyzed. This was done directly on a visual Hewlett-Packard chart recording. The same procedure for data reduction was used to measure the amplitude of waves corresponding to the first mode of the SOFAR signals recorded. In this case we measured the peak-to-peak amplitude of waves corresponding to the first normal mode as close to 20 Hz as possible. In some cases, in signals which traveled to ranges of more than 700 km, we had to measure the amplitude of waves of the first mode at a frequency as low as about 17 Hz because the 20 Hz waves were too weak. However, we will show later in this work, when we discuss the frequency dependence of the signal-to-noise ratios, that this frequency difference has a negligible effect on the measurements. The waves corresponding to the first mode were found to be the most useful ones for our analysis because they correspond to the most consistent and regular part of the Arctic SOFAR signal.

The observations of SOFAR signals recorded concurrently by geophones and by hydrophones have shown that there is considerable variability of up to about 20 DB in the differences of signal-to-noise ratios recorded by both types of sensors.

On the right side of Fig. 7 we show the histogram of the measured ratio in DB at 20 Hz of signal-to-noise of the hydrophone at a depth of 38 m in the water to that of the vertical-component geophone on the ice surface. These measurements were made from waves corresponding to the

first normal mode by the method described above. The distribution is not quite Gaussian. It displays a slight skew toward the higher ratios. We emphasize that the shots arrived during quiescent intervals of time between major tremor activity associated with strong local ice deformation. Small long-range shots were sometimes completely overwhelmed by the noise recorded by the geophones from this large-scale ice deformation, and thus they were useless for the analysis. In our data measured on sea ice near ice island T-3, we observed very poor signal-to-noise ratios of the geophones compared to the hydrophones (15 DB worse). We believe that this was caused by the fact that most of the signals were recorded during intervals of strong ice vibrations created by a very active pressure ridge 300 m away from the geophones. However, despite the poor performance of the geophones compared to the hydrophones observed near T-3, the ratio of the signal-to-noise of the vertical geophone when compared to that of the horizontal-radial geophone was about the same as we have commonly observed in other experiments (3-6 DB). The measurements made near T-3 suggest that the actual distribution may be bimodal, with one peak corresponding to quiescent intervals of ambient vibrations and a second one corresponding to listening conditions during active local ice deformation.

In Fig. 7, it is clear that a hydrophone at a depth of 38 m in the water of the channel is a far better listening device for SOFAR signals than a vertical geophone on the ice most of the time. About 80 percent of the signals cluster within the range of 5 to 9 DB. Occasionally (about 2 percent of the sample), the two sensors perform about equally well. The ice thicknesses at the geophone locations ranged between 2 and 12 m, although most of the measurements were made on sea ice about 3 m thick. We could not discern a clear trend in the differences of ratios as a function of ice thickness, and, as a matter of fact, the differences derived from data recorded near ARLIS II on ice between 10 and 12 m thick were on the average about the same as those measured on Station Charlie.

We cannot discern a seasonal dependence of the differences of the signal-to-noise ratios between the two sensors nor one dependent on geographic locations.

Despite the fact that the number of SOFAR signals recorded by horizontal-component geophones, is very small compared to the number recorded by vertical-component geophones, nevertheless, we followed the same procedure as for the vertical geophones for these signals, too. When the shots were not in line with the horizontal axis of the geophones, we derived the radial amplitude from the two orthogonal components; but because of the small number of shots recorded by horizontal-component geophones and the variability of differences in signal-to-noise ratios that we have observed from a large sample of SOFAR signals recorded by vertical-component geophones, we consider these data as merely an indication, as shown in Fig. 8, that the signal-to-noise ratios measured by the horizontal-component geophones when compared to those measured by the hydrophones will display considerable variability too.

Measurements in the infrasonic band below 10 Hz are difficult to make for three reasons.

First, the SOFAR signals are generally not well excited at frequencies below 8 Hz. Thus we have analyzed in some cases the bottom-interacting signals observed at long ranges over the abyssal plains. These signals are commonly very strong in the infrasonic frequency band from about 4 to about 15 Hz (Figs. 4a and 4b).

Second, pressure fluctuations induced by hydrophone cable strum can sometimes interfere strongly with the noise measurements recorded by hydrophones, and thus we could only analyze a limited number of signals in which we were certain that noise induced by hydrophone cable strum was negligible compared to the ambient noise field.

Finally, third, ambient ice vibrations near 2 Hz are commonly strong, and thus it is more difficult to locate shots in quiescent intervals in the ambient noise field than at higher frequencies.

Our first task was to locate SOFAR signals which were strongly excited in the infrasonic band from about 3 Hz to about 10 Hz. Fortunately, in our data recorded continuously for about 150 days, we located several signals of unknown origin recorded by both geophones and hydrophones which displayed strong waves corresponding to the first normal mode in the frequency band from about 3 Hz to about 15 Hz.

We next analyzed waves created by about 175 shots that we detonated in our experiments for frequency dependence. We analyzed shots recorded by both vertical and horizontal-radial geophones. In some of these signals we found an improvement of the geophones as listening devices relative to the hydrophones with decreasing frequency (Ref. 4), but on the average, little or no frequency dependence was observed in the band from about 8 Hz to about 20 Hz. We also observed in many shots a marked improvement of the hydrophone relative to the geophone below 7 Hz. In some cases, to extend the measurements below 10 Hz, we analyzed the bottom-interacting signals. We averaged the peak amplitudes in each octave band of several bottom-interacting pulses observed at long-ranges over the abyssal plains. Fig. 9 shows the distribution of the differences in signal-to-noise ratios of about 175 shots at 10 Hz. Fig. 10 shows the distribution of the differences in signal-to-noise ratios of 37 shots at 4 Hz. In Fig. 11, we observe that the average differences in the frequency band from 8 Hz to 20 Hz are nearly independent of frequency. At lower frequencies the performance of the hydrophone improves relative to the geophone approaching an average difference of 10 dB at 4 Hz. For the horizontal geophone the average differences are similar in character to those corresponding to the vertical geophone of Fig. 11, but they are about 3 dB higher than that shown in Fig. 11.

The theoretical ratios shown in Table I were derived from transmission loss computations made by the FFP. The "minimum ratio" corresponds to the lowest noise spectrum levels of ice vibrations measured by Prentiss et al. (Ref. 5) and the minimum water noise measured by Mellen and Marsh (Ref. 6), and the "maximum ratio" corresponds to the maximum noise levels measured by these researchers for both ice vibrations and noise in the water of the channel. We note in Table

I that the performance predicted for the hydrophone, as compared to that of the vertical geophone, agrees reasonably well with the measurements, but that there is a marked discrepancy with data for the horizontal geophone (Fig. 8).

Signal-to-Noise: SOFAR Signals Compared to Seismic Waves

Differences in signal-to-noise ratios between hydrophones and geophones were measured as a function of signal grazing angle with level ice and signal frequency. Fig. 7 shows that as a function of grazing angle at 20 Hz the frequency distributions in the differences clearly define two groupings. One group represents waves traveling in the Arctic sound channel with grazing angles less than 20 degrees and the other group represents waves with large grazing angles beyond 70 degrees such as long-range mantle P and S waves created by earthquakes and explosions, (Fig. 12 & 13). Fig. 7 shows that at 20 Hz in SOFAR signals, T-phases, and topographic echoes the hydrophones at depths near 40 m in the water of the channel record waves about 7 dB stronger in average signal-to-noise ratio compared to the vertical geophones on the ice, while at large grazing angles near 75 degrees the relative performance between the two sensors reverses, with the average signal-to-noise ratio recorded by the vertical geophones about 3 dB better compared to that recorded by the hydrophones. Figs. 11 and 14 show that the average differences in signal-to-noise ratios between the hydrophones and the geophones are nearly independent of frequency in the band from 8 Hz to 20 Hz in both groups of waves, but that at lower frequencies in both groups of waves the performance of the hydrophones improves relative to the geophones, approaching an average difference of 10 dB at 4 Hz.

Particle Motions

Signals recorded by horizontal geophones are far more sensitive to ice conditions near the listening sites than signals recorded concurrently by hydrophones or by vertical geophones. In order to estimate the reliability of theoretical predictions of particle motions computed from a model consisting of a flat plate resting on the Arctic channel, we conducted a series of experiments to measure the ratio of horizontal particle velocity in the radial direction to vertical velocity as a function of KH/2, where K is the horizontal wavenumber and H is the plate thickness, (Fig. 15).

Plate thicknesses ranged between 2m and 25m, wave frequencies ranged between 5 Hz and 500 Hz, and phase velocities ranged between 300 m/sec and 1200 m/sec in flexural waves and between 1437 m/sec and 10,000 m/sec in waves propagating in the Arctic channel (grazing angles with the ice between 3 degrees and 85 degrees).

The analysis of these data is shown in Fig. 16. Fig. 16 shows that we can expect reasonable agreement between field data and theoretical predictions in the range of KH/2 between about .4 and about 2. At smaller KH/2 the horizontal particle velocities are up to 30 dB stronger than those predicted and these motions appear to be strongly controlled by local large-scale irregularities on the plate boundaries such as hummocks, pressure ridges, and leads, while at larger KH/2,

irregularities in the ice near the seismic array strongly scatter waves producing a long-duration incoherent vibration (coda) with the strongest amplitudes on the horizontal components of motion, (Fig. 17).

When a flat plate of ice is introduced at the surface of the Arctic channel, the numerical computations predict a phase difference of $\pm$ 90 degrees between the horizontal radial and the vertical particle velocities at the surface of the ice at each range point. This corresponds in waves trapped in the channel to a retrograde elliptical particle motion, similar to that observed in ordinary flexural waves in the ice. Figs. 18 and 19 show that this type of vibration with the above characteristics is observed in field data since the vertical motion of the bottom-interacting pulse recorded by a 3-component seismograph on the ice surface is approximately the Hilbert transform (90 degree phase difference) of the horizontal radial motion and the particle orbit is a retrograde elliptical one. Fig. 20 shows the 90 degree phase difference in the computed waveforms of the bottom interacting signals.

Suggestions for Future Work

1. Extend the FFP computer code to compute transmission loss of ice vibrations on a rough plate resting on the Arctic channel because clearly the present theory does not model the horizontal vibration levels.

2. Conduct an extensive set of experiments with linear seismic and hydrophone arrays with the purpose to measure differences of signal-to-noise ratios and ratios of horizontal to vertical particle velocity and phase differences as a function of signal frequency, grazing angle, and ice thickness. Experiments would be conducted at long ranges between two quiet ice stations along paths over an abyssal plain to record measurements of bottom-interacting pulses as well as SOFAR signals, (Figs. 4a and 4b).

References

1. Kutschale, H.W., Arctic Marine Acoustics, Final Report under Contract N00014-80-C-0021, Lamont-Doherty Earth Observatory of Columbia University, Palisades, NY, 1984.

2. Kutschale, Henry, Long-Range Sound Transmission in the Arctic Ocean, J. Geophys. Res., 66(7), 2189-2198, 1961.

3. Kutschale, H.W., Low-Frequency Acoustic Wave Propagation, Final Report under Contract N660489-M-B005, Lamont-Doherty Earth Observatory of Columbia University, Palisades, NY, 1990.

4. Kutschale, H.W., Low-Frequency Ice Vibrations on the Arctic Channel: Propagation and Ambient Noise, Final Report under Contract N00014-85-K-2009, Lamont-Doherty Earth Observatory of Columbia University, Palisades, NY, 1986.

5. Prentiss, David, Edward Davis, and Henry Kutschale, Natural and Man-Made Ice Vibrations in the Central Arctic Ocean in the Frequency Range from 0.1 to 100 cps, Tech. Rep. No. 4, CU-4-65-Nonr 266 (82), Lamont-Doherty Earth Observatory of Columbia University, Palisades, NY, pp.54, 1965.

6. Mellen, R.H. and H.W. Marsh, Underwater Sound in the Arctic Ocean, Report MED-65-1002, U. S. Navy Underwater Sound Lab, New London, CT, 1965.

Table I

COMPUTED RATIO OF SIGNAL-TO-NOISE RATIOS AT 10 Hz

OF A HYDROPHONE AT 50 m TO A GEOPHONE AT ICE SURFACE

Vertical Geophone

MIN	MAX
5 db	12 db

Horizontal-Radial Geophone

MIN	MAX
30 db	37 db

Figure Captions

Fig. 1 Typical ray paths in the Arctic Channel.

Fig. 2 Typical SOFAR signal displaying marked frequency dispersion.

Fig. 3 Typical SOFAR signals recorded simultaneously by hydrophones and by vertical-component geophones.

Fig 4a Temporal waveforms recorded by a hydrophone at depth in the Arctic channel and by a geophone on the ice surface.

Fig 4b Sound spectrograms of the signals shown in Fig. 4a.

Fig 5 Sound spectrogram of waveform shown in Fig. 2. Dispersion of first and second mode is clearly shown.

Fig. 6 Simultaneous recordings of ambient noise by a vertical-component geophone on the ice and by a hydrophone at depth of about 50 m in the channel. Frequency band is 1 to 80 Hz.

Fig. 7 Histograms of differences of signal-to-noise ratios between hydrophones and vertical geophones.

Fig. 8 Histogram of ratio of signal-to-noise ratios of a hydrophone at a depth of 38 m in the water to a horizontal-radial geophone on the ice surface. Frequency 20 Hz.

Fig. 9 Histogram of ratio of signal-to-noise ratios of a hydrophone at a depth of 38 m in the water to a vertical-component geophone on the ice surface. Frequency 10 Hz.

Fig. 10 Histogram of differences of signal-to-noise ratios between a hydrophone and a vertical geophone at 4 Hz.

Fig. 11 Average difference of signal-to-noise ratios between a hydrophone and a vertical geophone for SOFAR signals as a function of frequency.

Fig. 12 Long-range signal created by an explosion. Frequency band 10 to 20 Hz.

Fig. 13 Typical signal created by an earthquake on the Arctic Mid-Ocean Ridge. Mean horizontal velocities of waves corresponding to P, S and T are 7.2 km/sec, 4.2 km/sec, and 1.47 km/sec, respectively.

Fig. 14 Average differences of signal-to-noise ratios between hydrophones and geophones of seismic signals at large grazing angles. Average is composed of 37 signals.

Fig. 15 Diagram of experiment.

Fig. 16 Comparison as a function of KH/2 of measured ratios of horizontal to vertical particle velocity at ice surface with that computed by thin plate theory. Above KH/2 = .5 the curve is computed by Timoshenko-Mindlin theory.

Fig. 17 Temporal waveforms of bottom-interacting signals observed over the Chukchi Abyssal Plain. These waveforms were measured by a 3-component geophone array.

Fig. 18 Temporal waveforms of bottom-interacting signal. These waves were recorded by a 3-component geophone array on the ice surface. Grazing angle with the surface is about 29 degrees.

Fig. 19 Particle motion at 50 Hz in bottom-interacting signal at a grazing angle with the ice of about 29 degrees.

Fig. 20 Temporal waveforms of bottom-interacting pulses computed by the FFP as a function of range. Source is a single cycle of an 8 Hz sine wave. Velocity scale of the vertical motion is 10 times that of the horizontal radial motion; i.e. the ratio of the vertical to horizontal particle velocity is 10. Water depth 4.2 km.

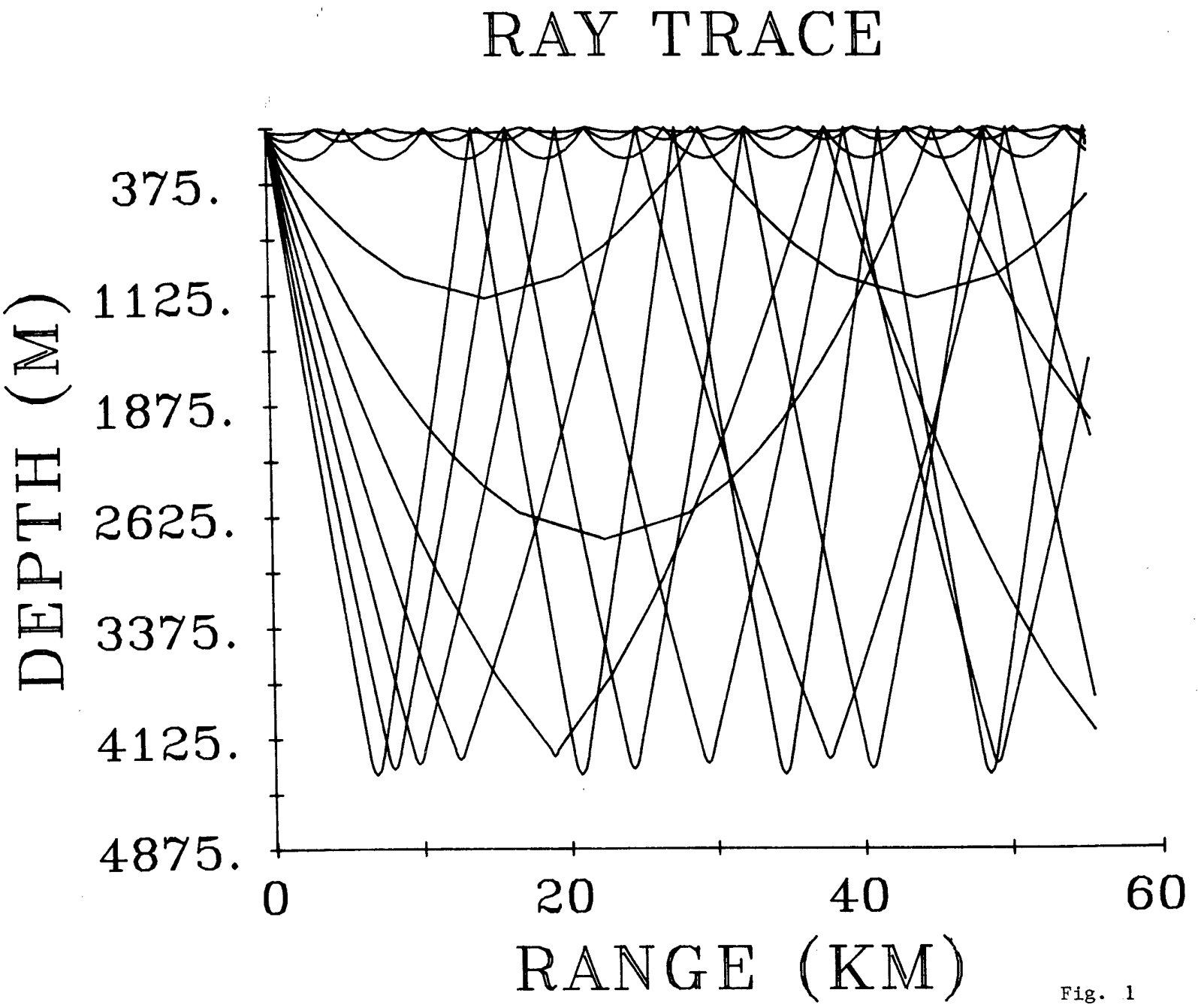
RAY TRACE
DEPTH (M)
375.
1125.
1875.
2625.
3375.
4125.
4875.
0
20
40
60
RANGE (KM)

Fig. 1

FRAM I '79
HYDROPHONE at 175 Ft
CHARGE SIZE: 55 lbs
SHOT DEPTH: 800 Ft
RANGE: 720 Km

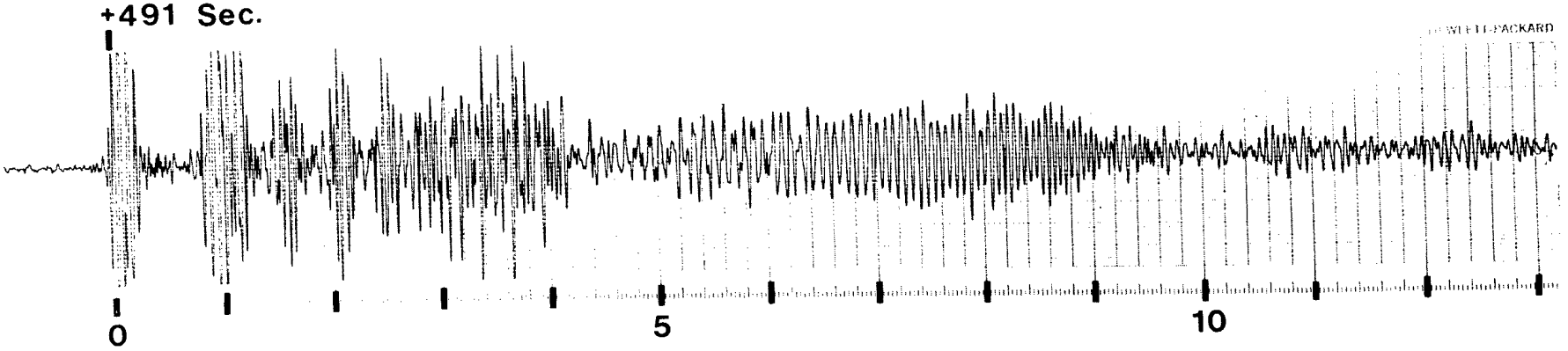

Fig. 2

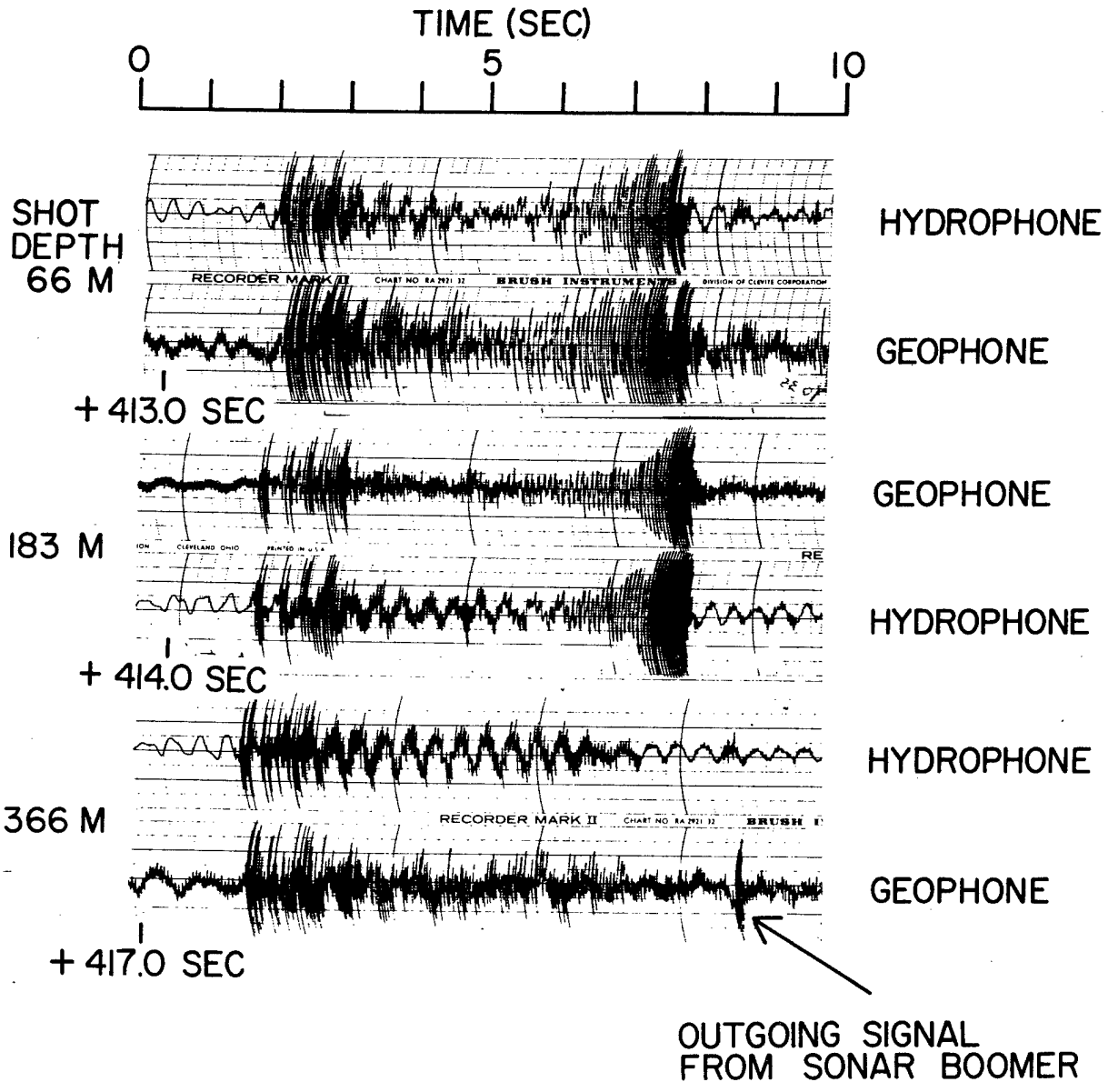
TIME (SEC)
0
5
10
SHOT DEPTH 66 M
HYDROPHONE
GEOPHONE
+ 413.0 SEC
GEOPHONE
183 M
HYDROPHONE
+ 414.0 SEC
HYDROPHONE
366 M
GEOPHONE
+ 417.0 SEC
OUTGOING SIGNAL FROM SONAR BOOMER

Fig. 3

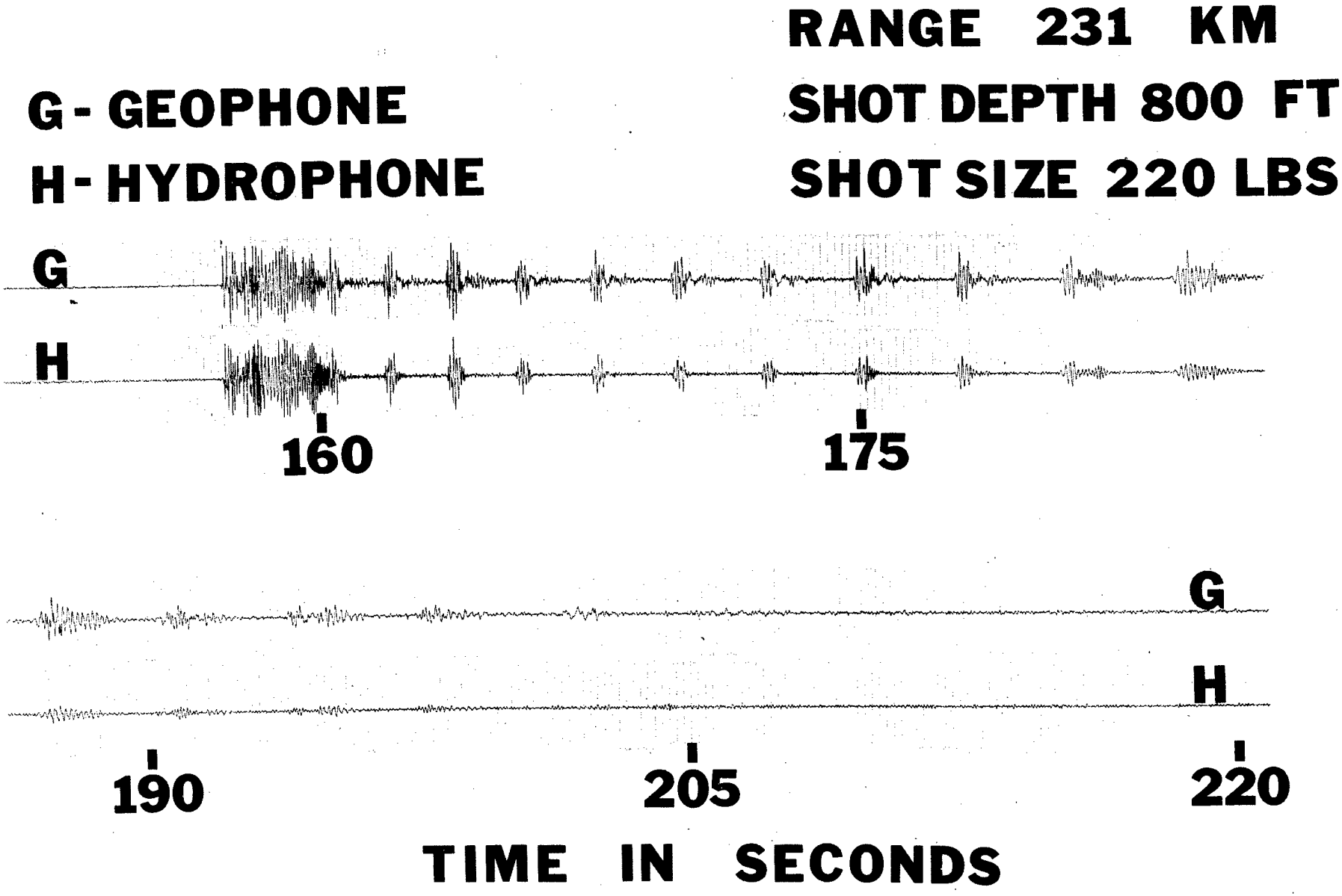
RANGE 231 KM
G - GEOPHONE
H - HYDROPHONE
SHOT DEPTH 800 FT
SHOT SIZE 220 LBS
G
H
160
175
G
H
190
205
220
TIME IN SECONDS

Fig. 4a

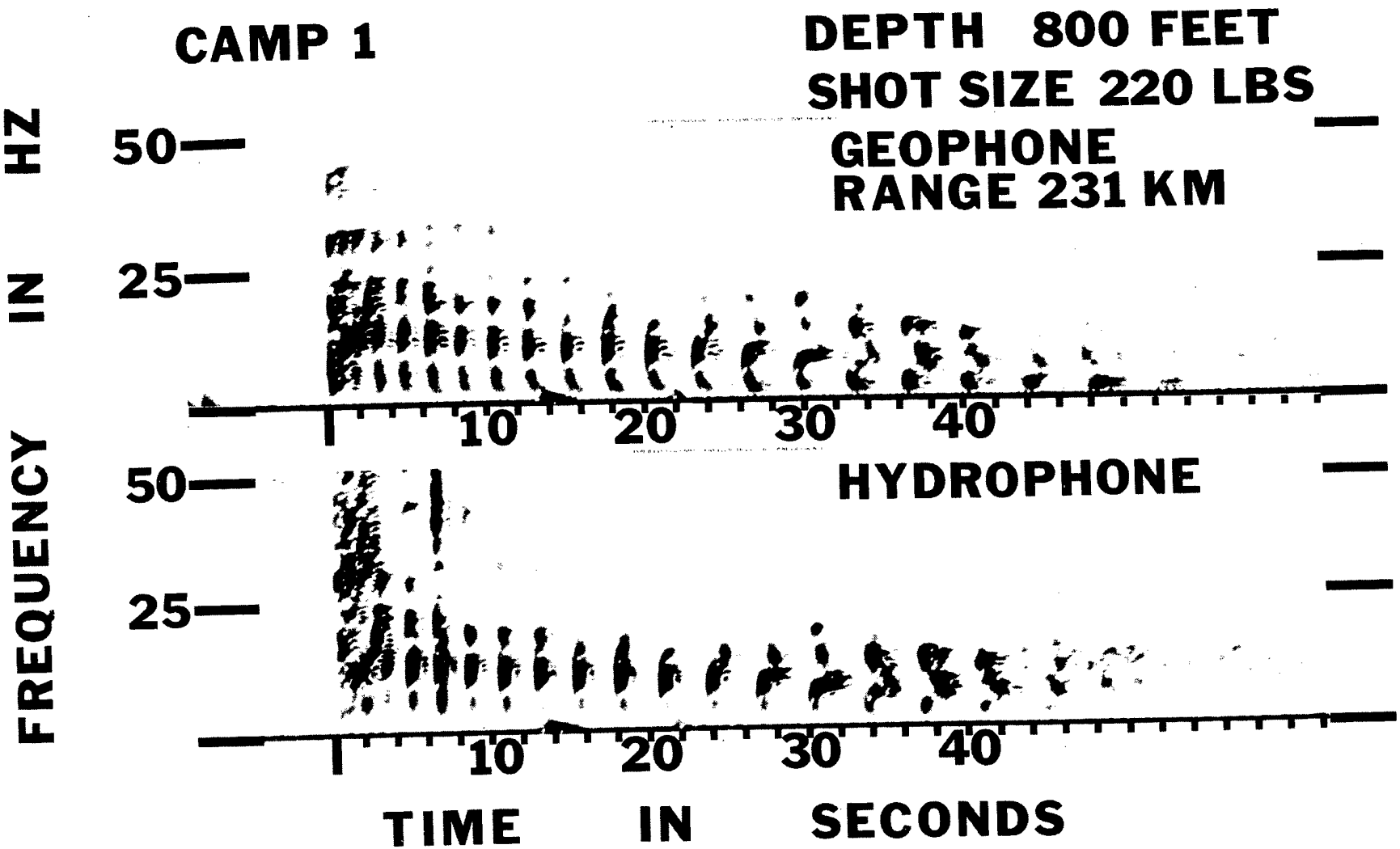
CAMP 1
DEPTH 800 FEET
SHOT SIZE 220 LBS
GEOPHONE
RANGE 231 KM
FREQUENCY IN HZ
50
25
10
20
30
40
HYDROPHONE
TIME IN SECONDS

Fig. 4b

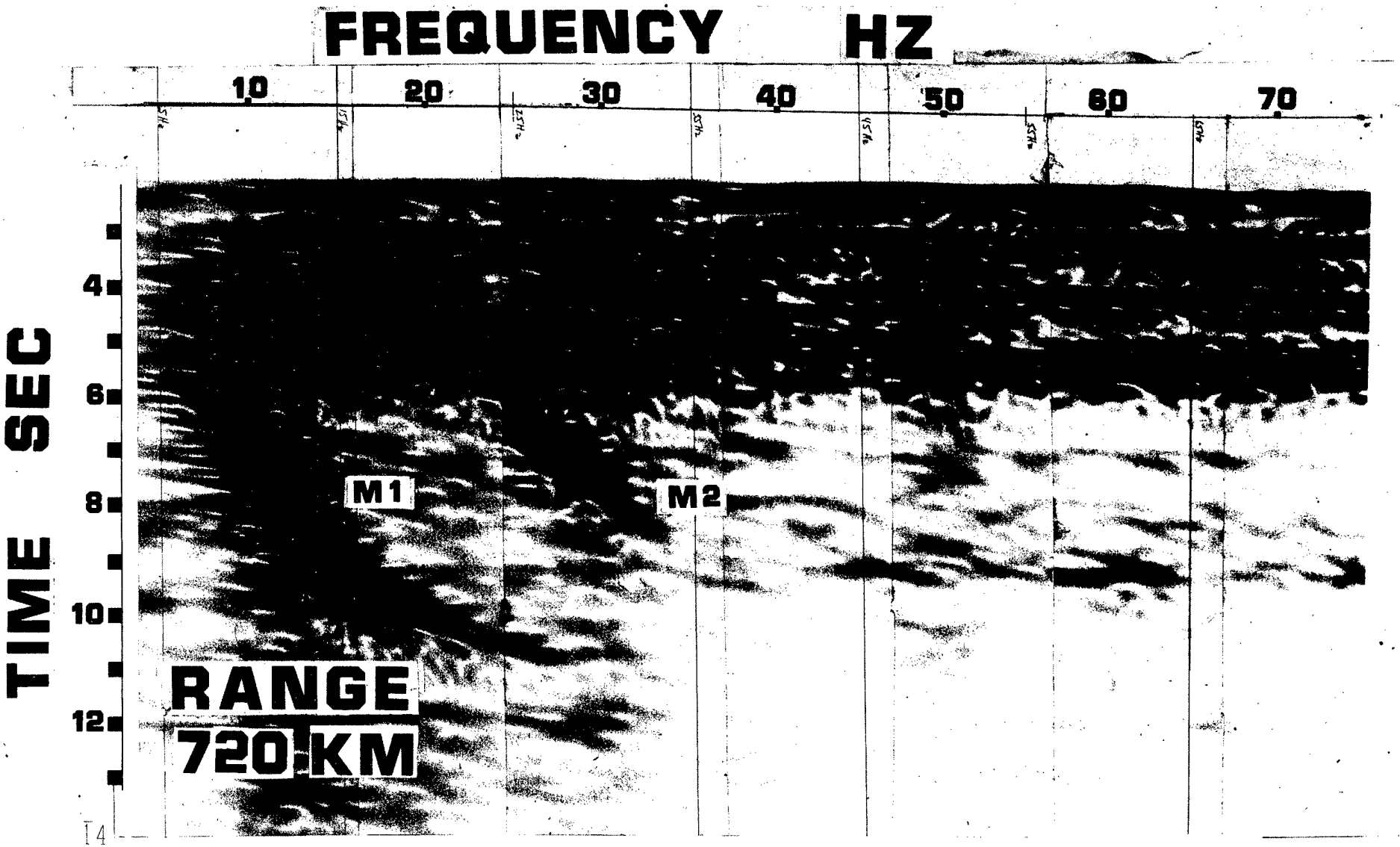
FREQUENCY HZ
10
20
30
40
50
60
70
TIME SEC
4
6
8
10
12
M1
M2
RANGE
720 KM

Fig. 5

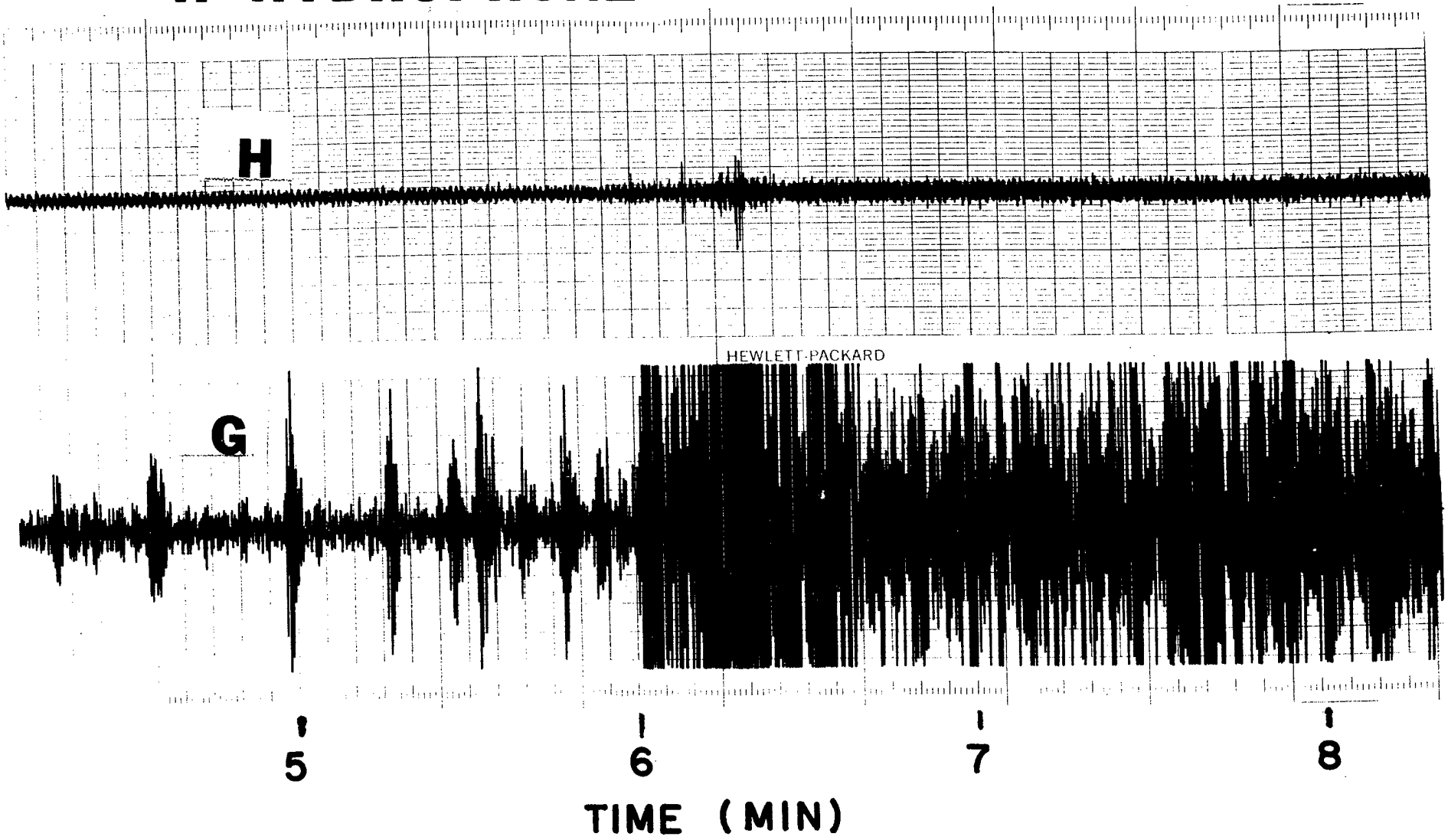

Fig. 6

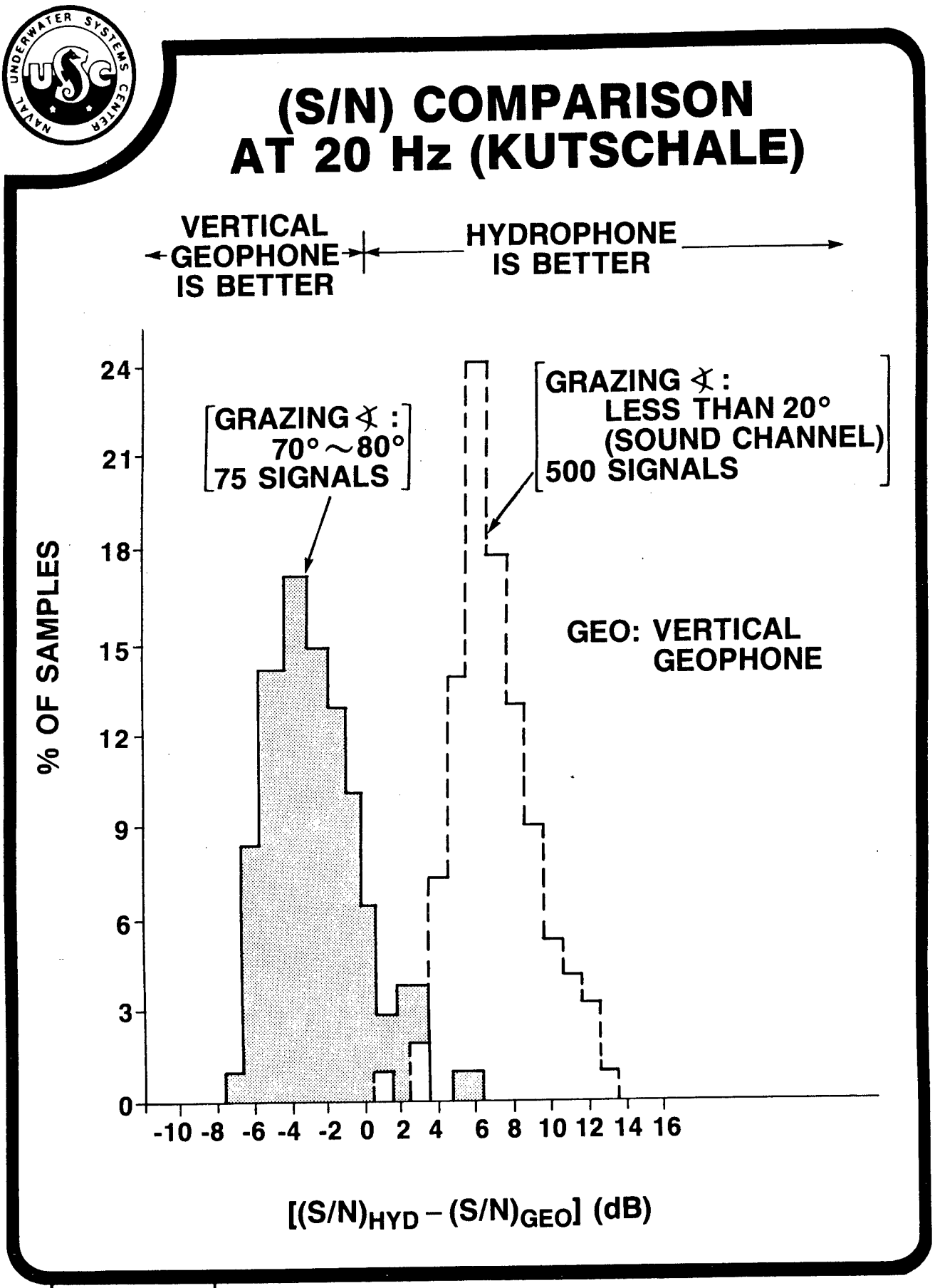

N0211-GA-89(L)-01483.2E

Fig. 7

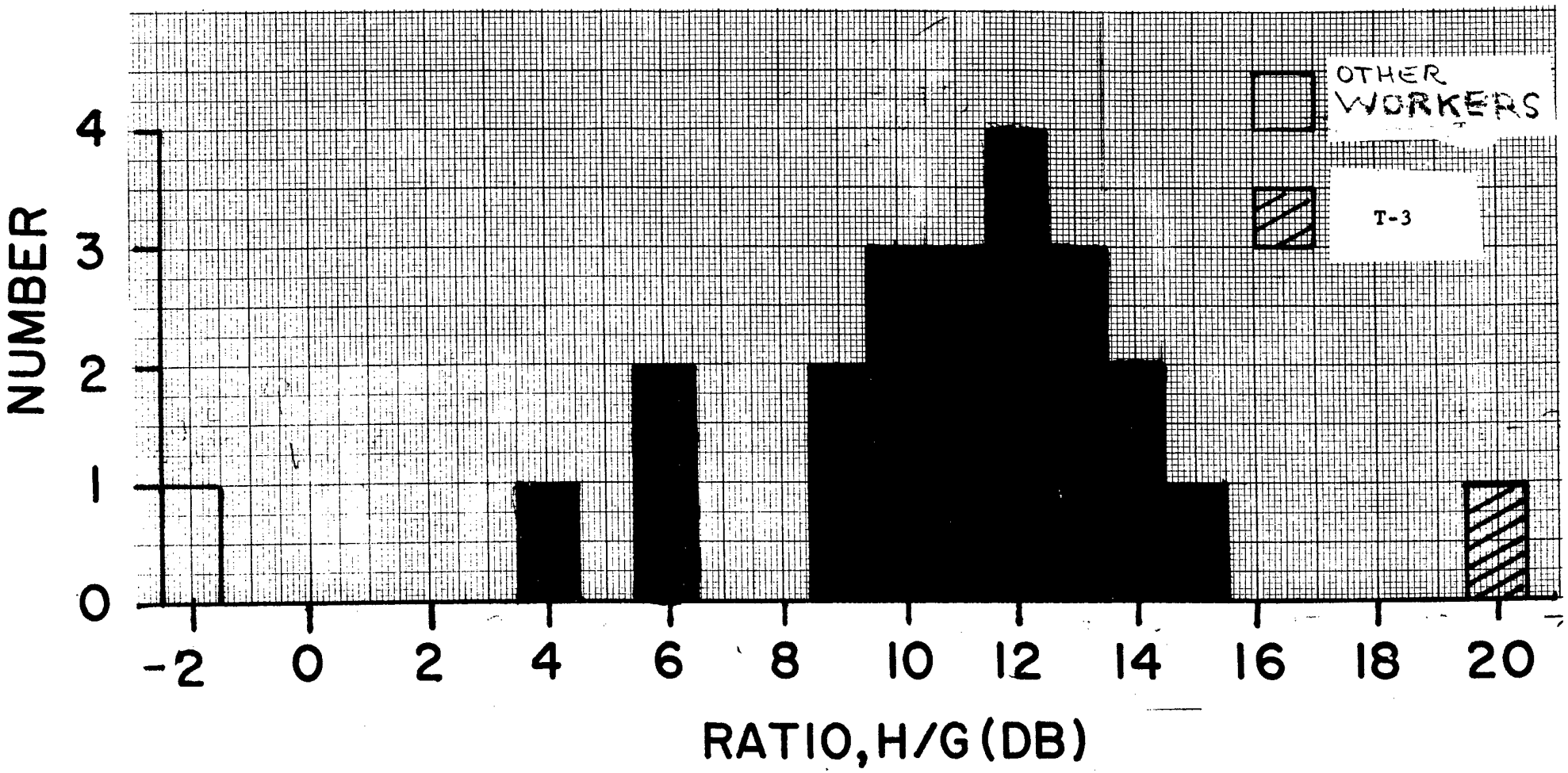

G - GEOPHONE

H - HYDROPHONE

Fig. 8

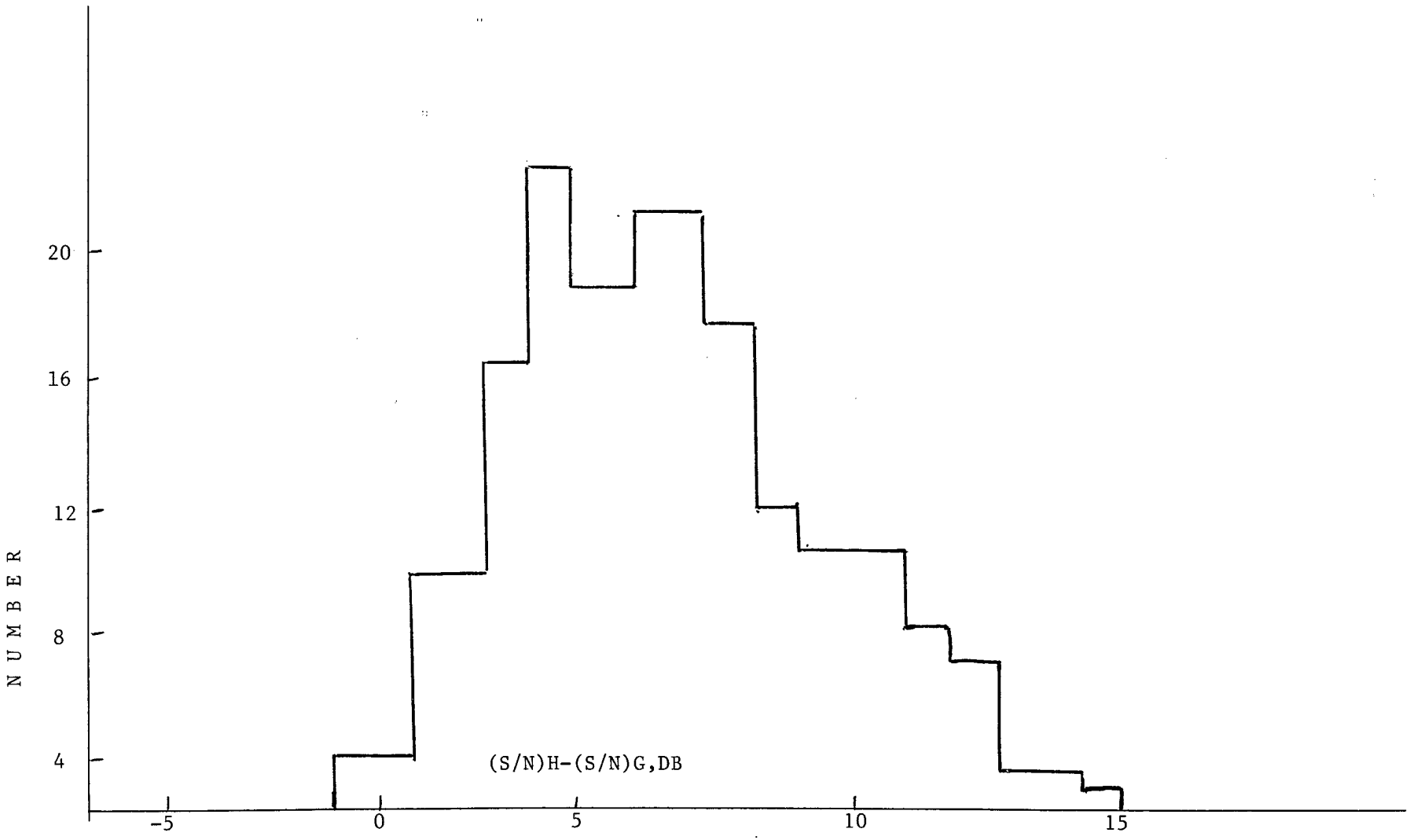

Fig. 9

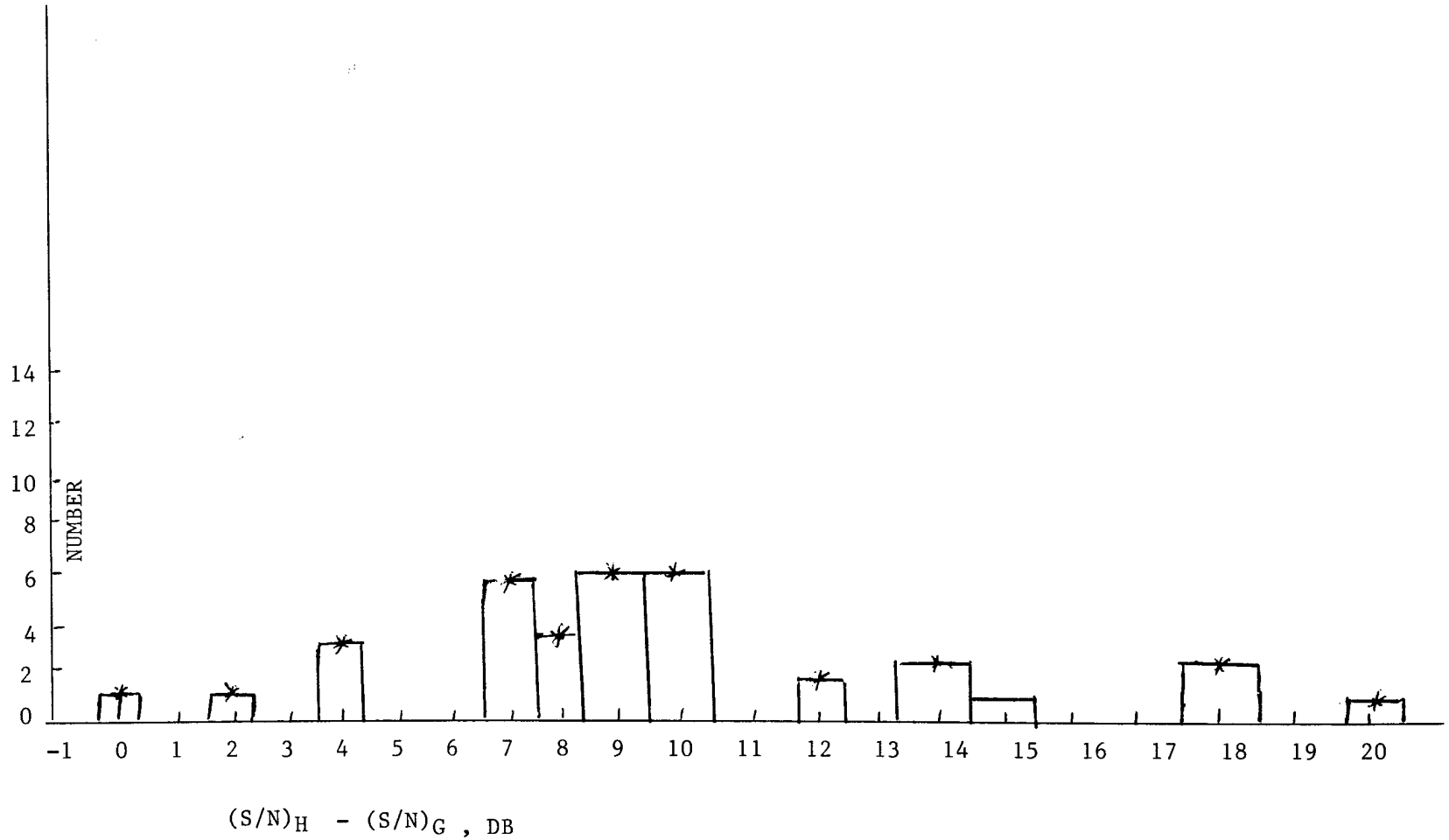
NUMBER
14
12
10
8
6
4
2
0
-1 0 1 2 3 4 5 6 7 8 9 10 11 12 13 14 15 16 17 18 19 20
(S/N)H - (S/N)G , DB

Fig. 10

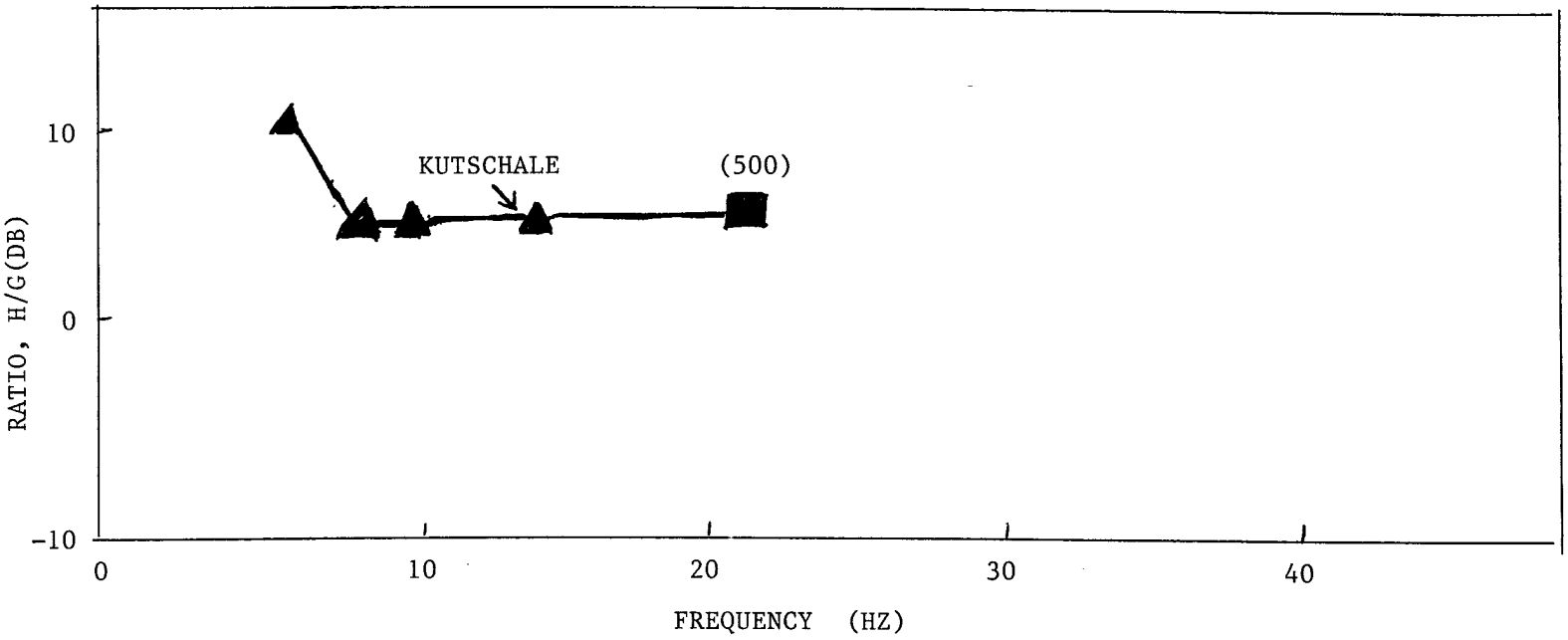

Fig. 11

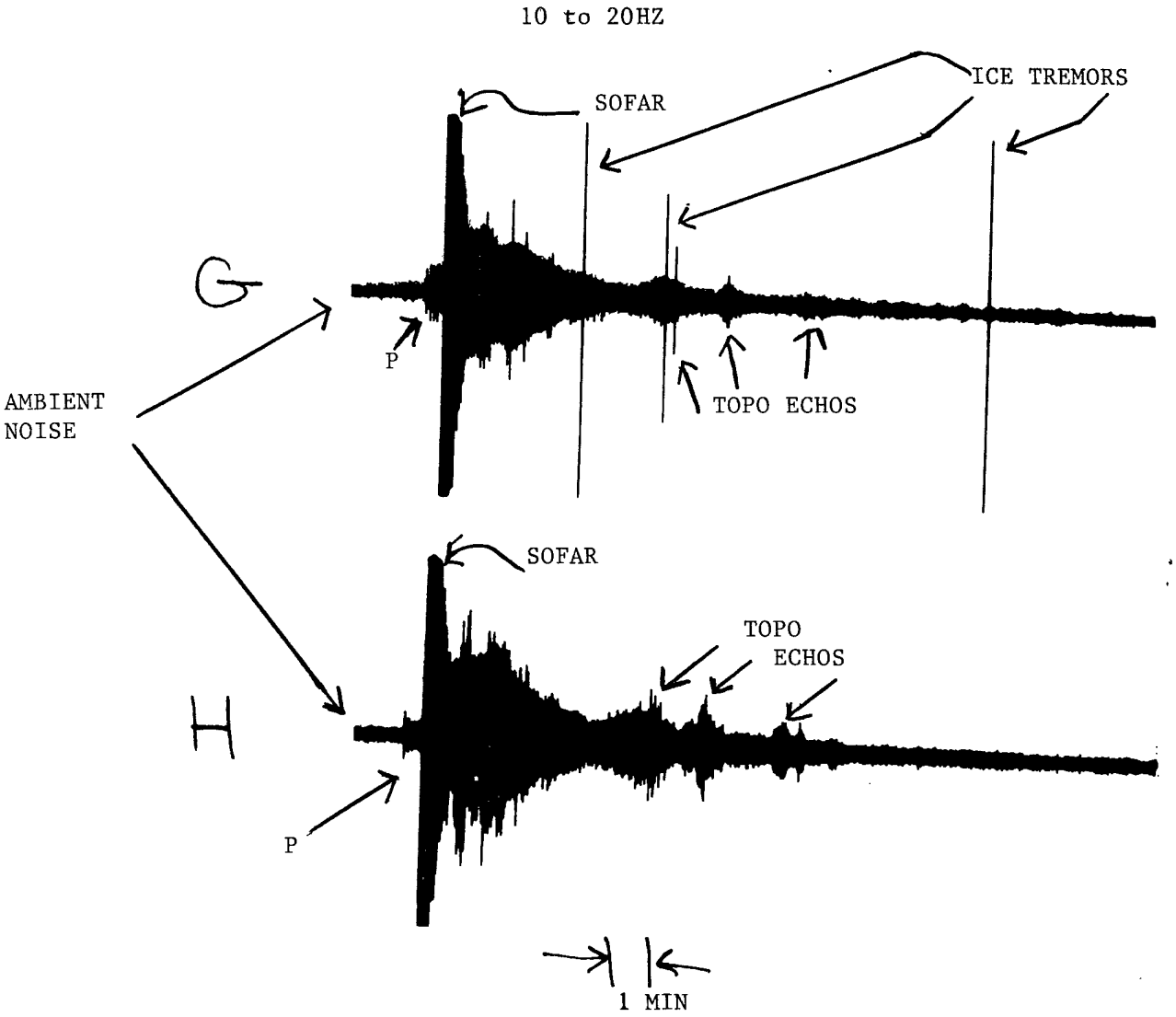
10 to 20HZ
ICE TREMORS
SOFAR
G
P
AMBIENT
NOISE
TOPO ECHOS
SOFAR
TOPO
ECHOS
H
P
1 MIN

Fig. 12

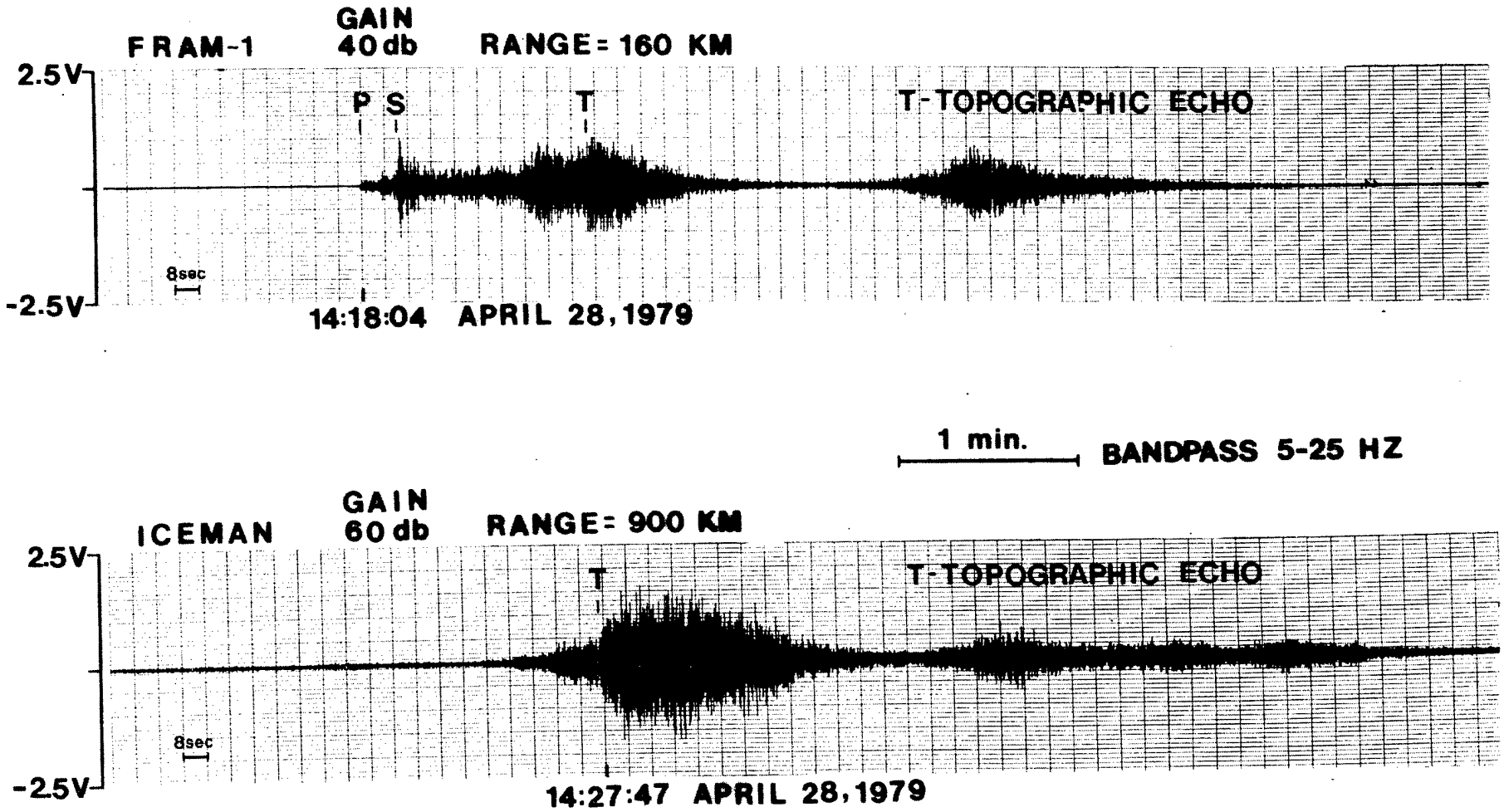
FRAM-1
GAIN
40 db
RANGE = 160 KM
2.5V
P
S
T
T-TOPOGRAPHIC ECHO
8sec
-2.5V
14:18:04 APRIL 28, 1979
1 min.
BANDPASS 5-25 HZ
ICEMAN
GAIN
60 db
RANGE = 900 KM
2.5V
T
T-TOPOGRAPHIC ECHO
8sec
-2.5V
14:27:47 APRIL 28, 1979

Fig. 13

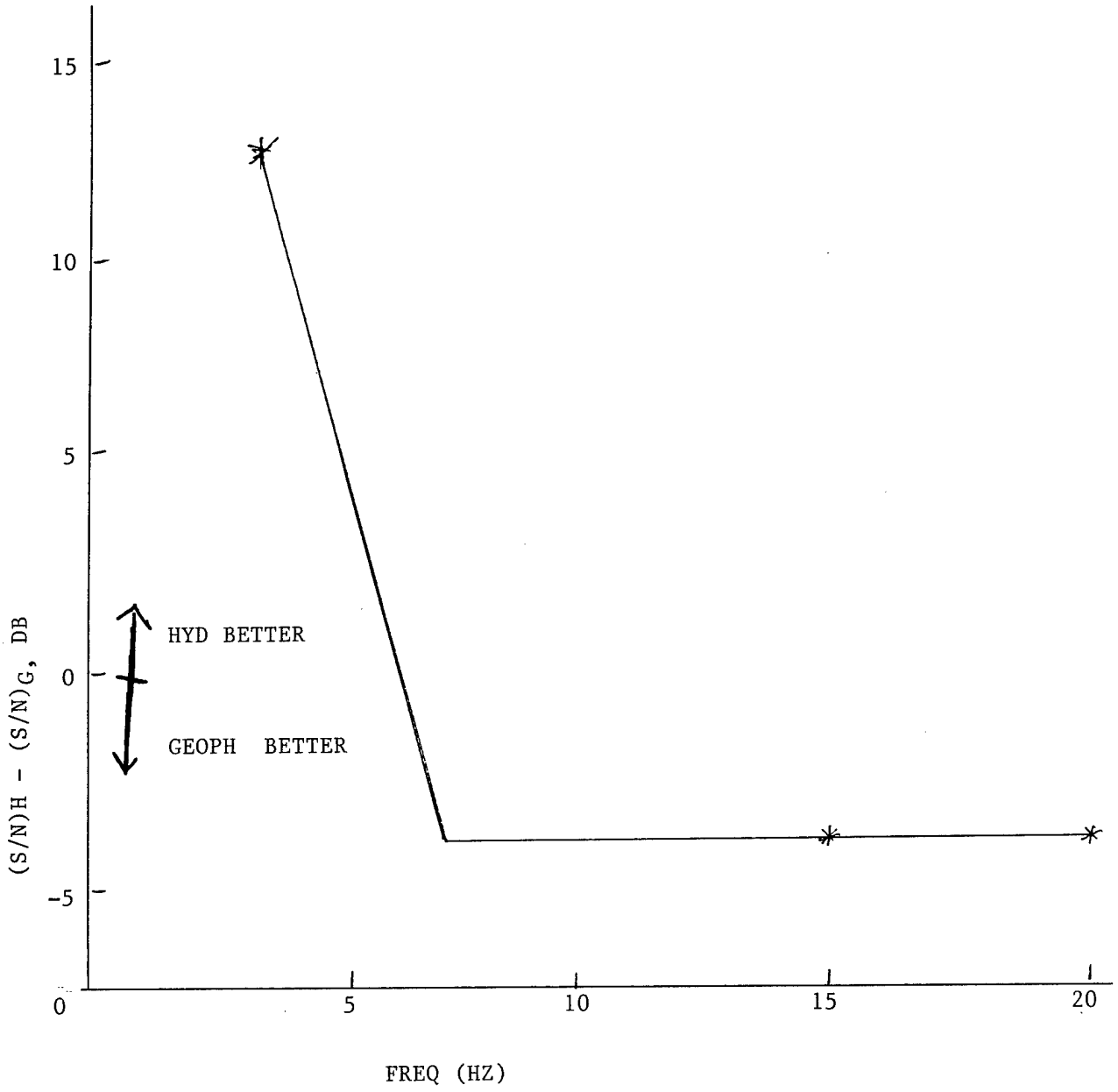

Fig. 14

MEASURE RATIO $\left| \text{HOR}/_{\text{VERT}} \right| e^{i\phi}$ AS A

FUNCTION OF $\frac{KH}{2} = \frac{W}{C} H/2 = \frac{2\pi H}{\lambda} / 2$

C = HORIZONTAL PHASE VELOCITY

λ = HORIZONTAL WAVELENGTH

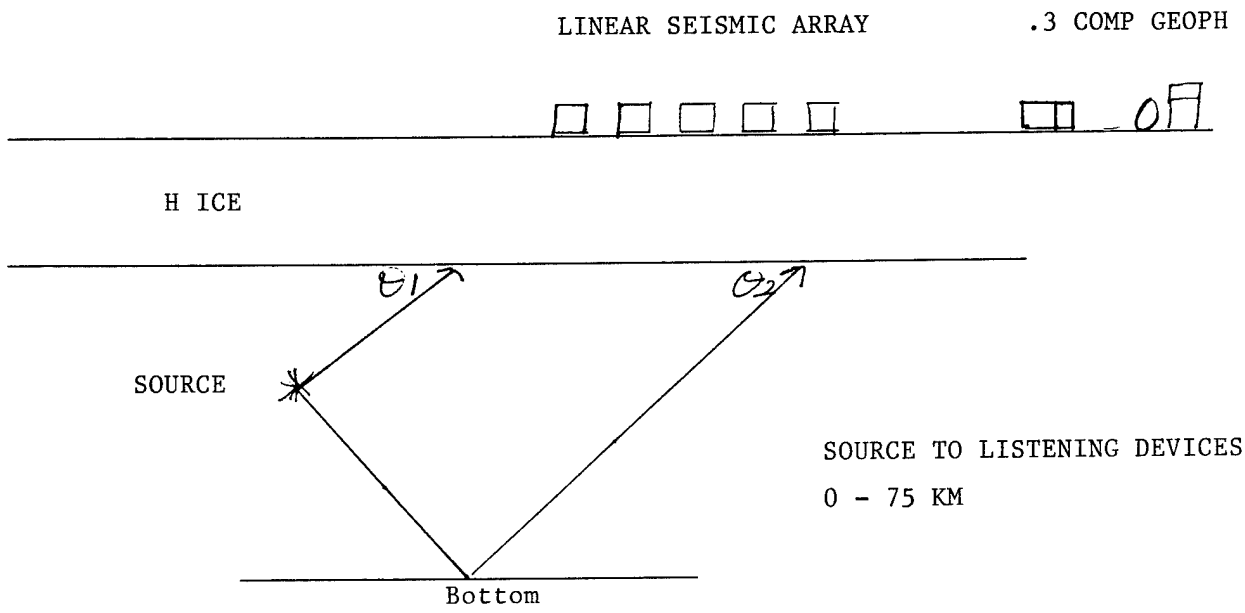

Fig. 15

AN ICE VIBRATION ANOMALY (KUTSCHALE)

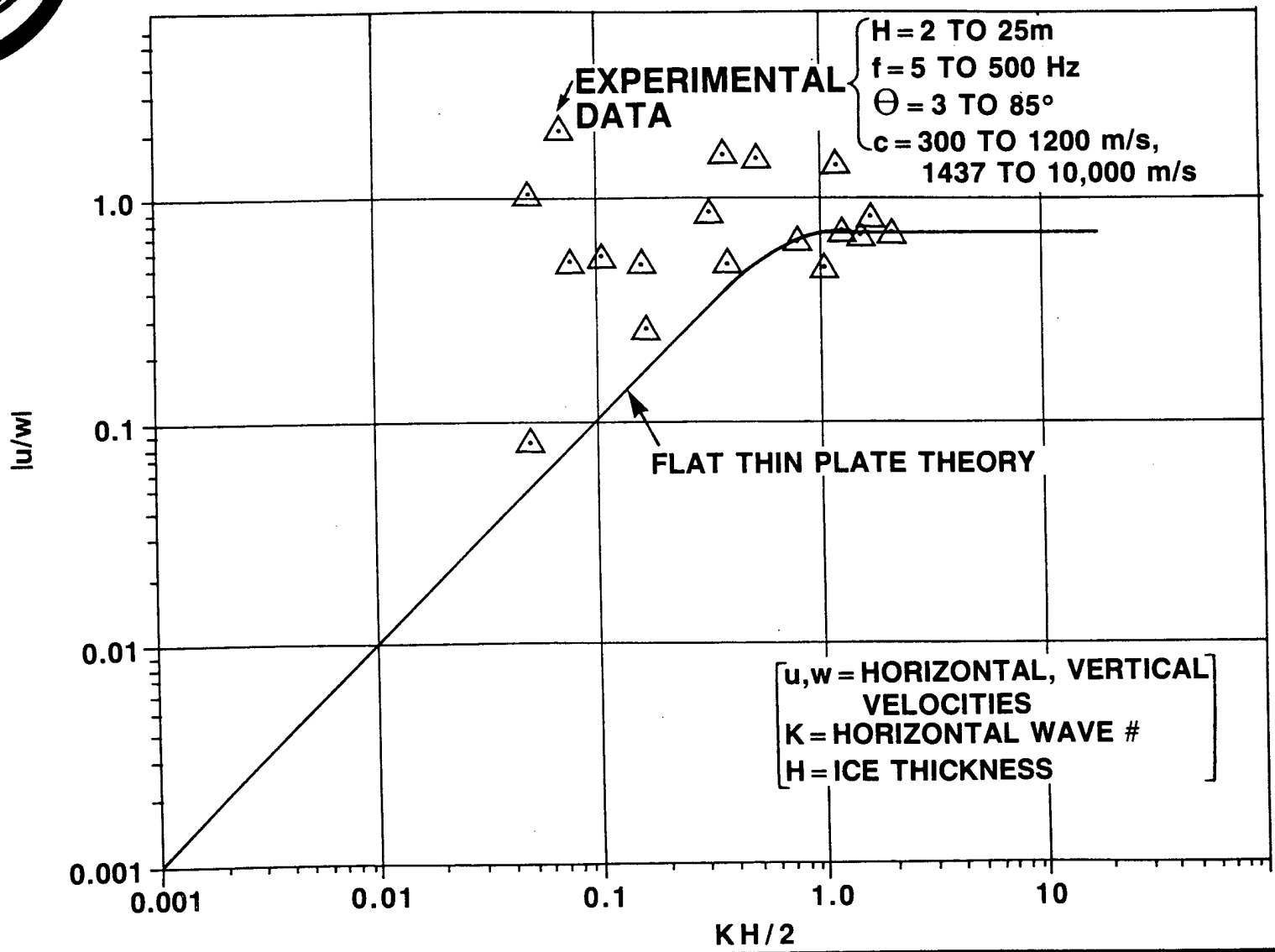

N0211-GA-89(L)-01483.6E

Fig. 16

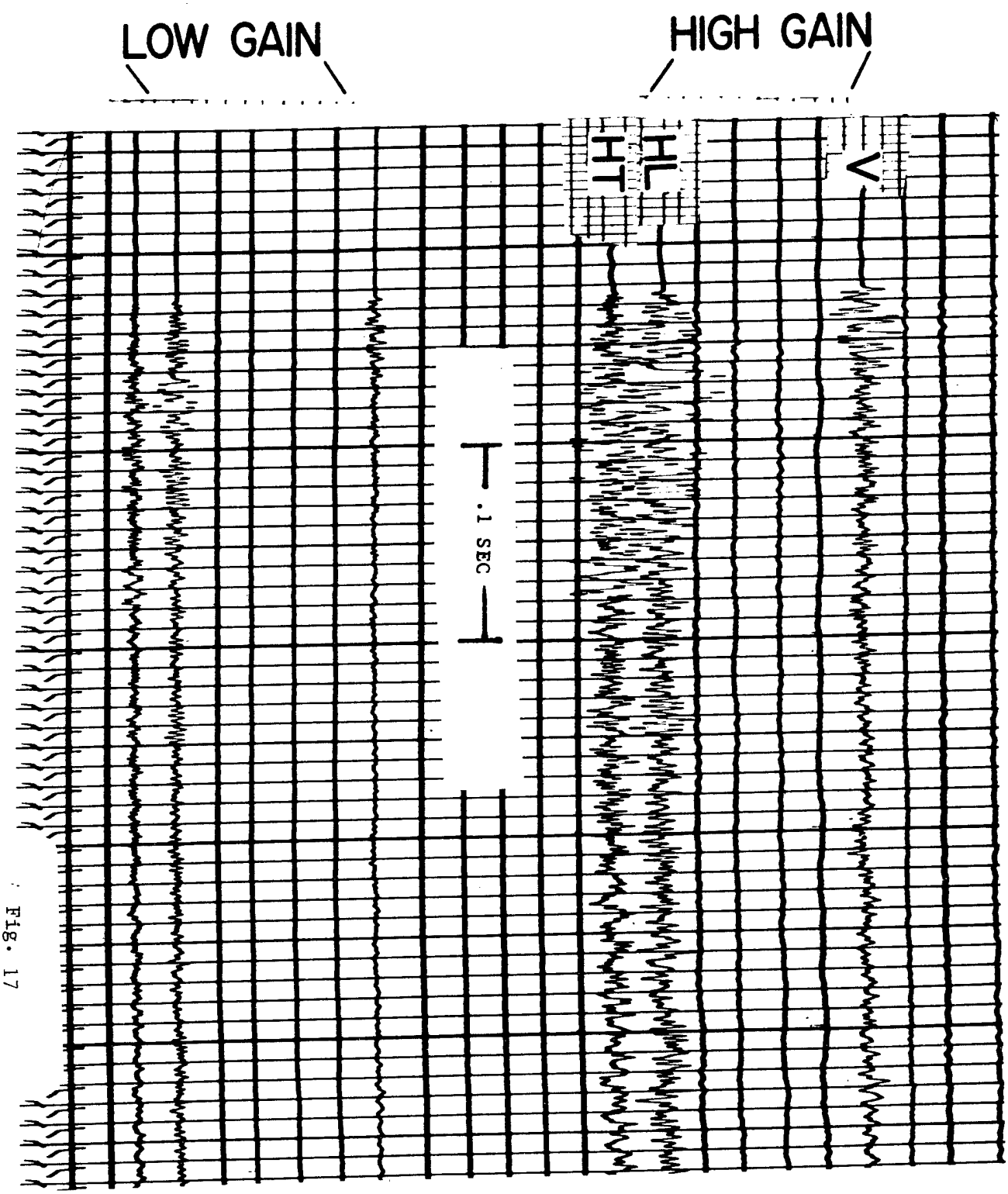

Fig. 17

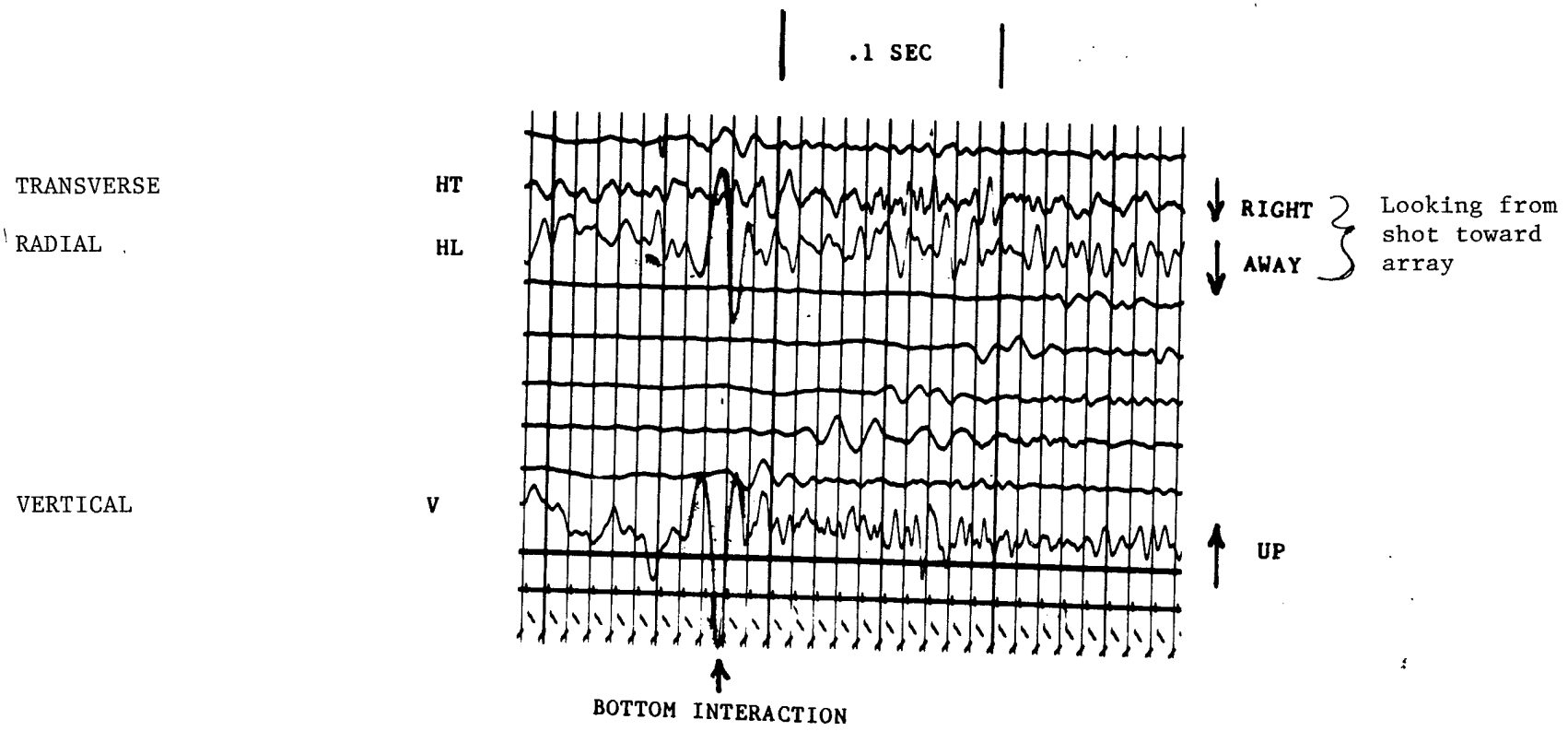
.1 SEC
TRANSVERSE
HT
RADIAL
HL
VERTICAL
V
RIGHT
AWAY
Looking from shot toward array
UP
BOTTOM INTERACTION

Fig. 18

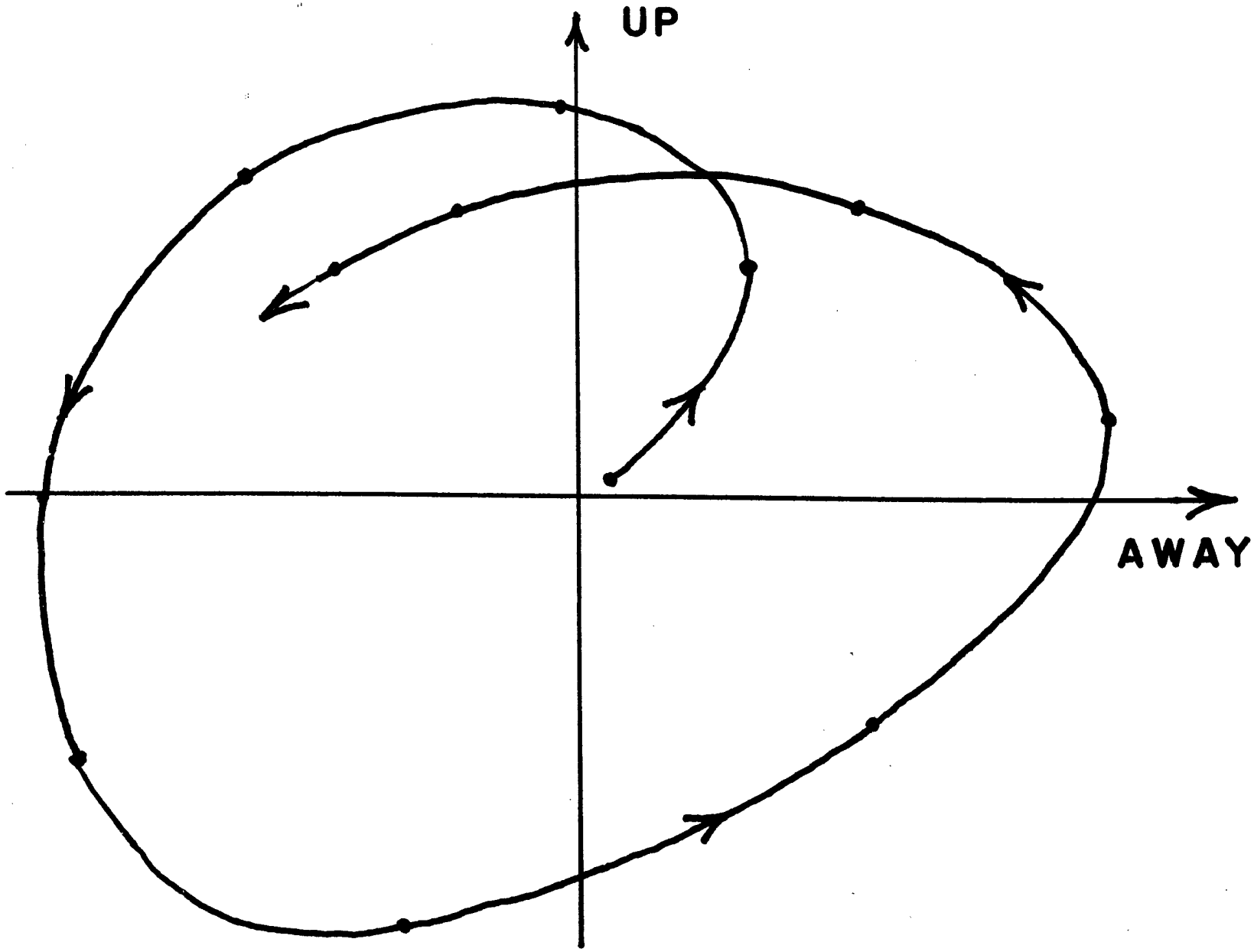

Fig. 19

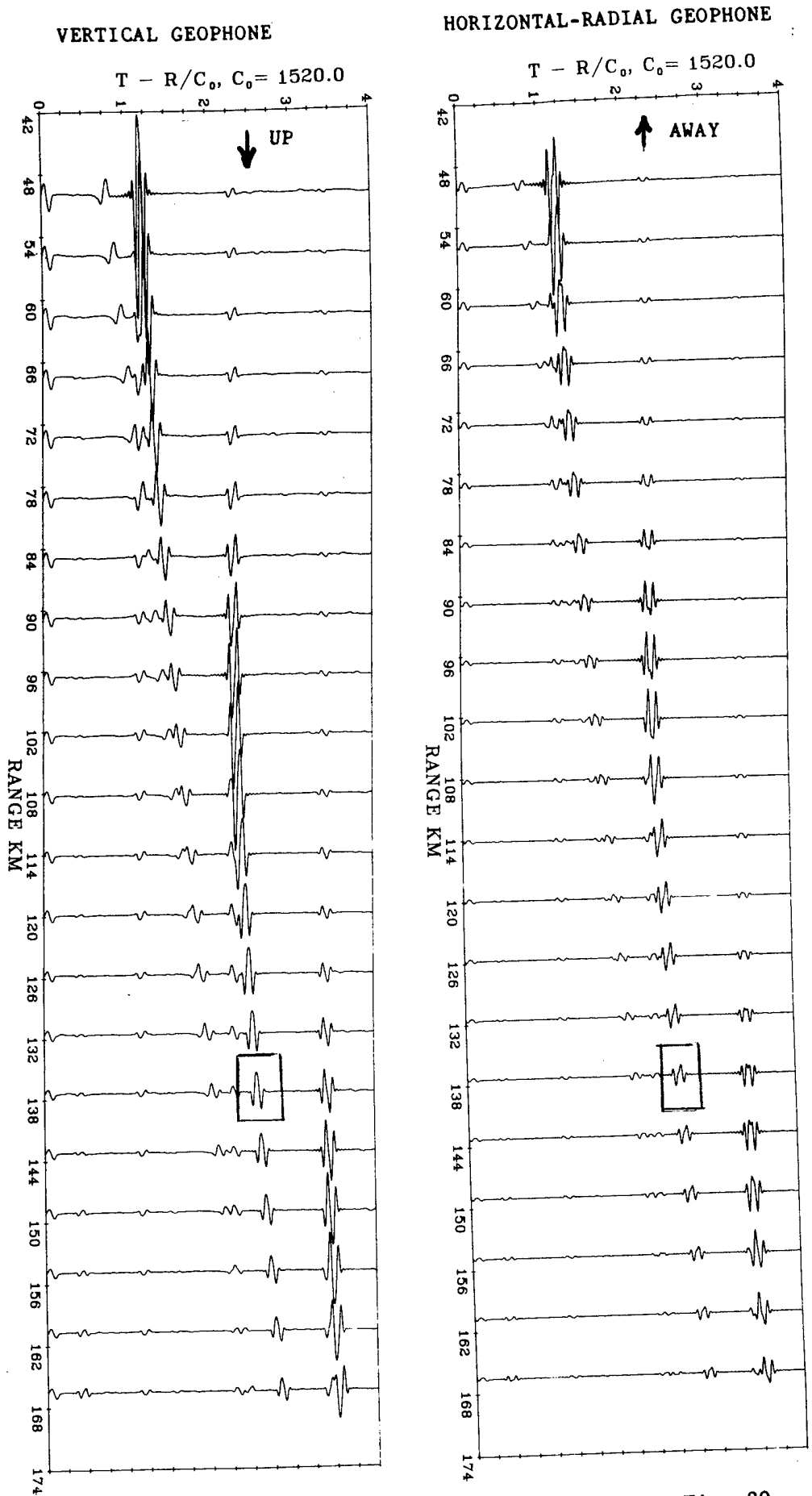
VERTICAL GEOPHONE
T − R/C₀, C₀= 1520.0
UP
RANGE KM
HORIZONTAL-RADIAL GEOPHONE
T − R/C₀, C₀= 1520.0
AWAY
RANGE KM

Fig. 20